

**PHYSICAL AND FUNCTIONAL INTERACTIONS OF
TWO NATURALLY-OCCURRING MUTANT VARIANTS OF THE P2Y12
RECEPTOR**

by

Cara Giordano

A thesis submitted to the Faculty of the University of Delaware in partial fulfillment of the requirements for the degree of Master of Science in Biological Sciences

Summer 2019

© 2019 Cara Giordano
All Rights Reserved

**PHYSICAL AND FUNCTIONAL INTERACTIONS OF
TWO NATURALLY-OCCURRING MUTANT VARIANTS OF THE P2Y₁₂
RECEPTOR**

by

Cara Giordano

Approved: _____
Donna S. Woulfe, Ph.D.
Professor in charge of thesis on behalf of the Advisory Committee

Approved: _____
Velia Fowler, Ph.D.
Chair of the Department of Biological Sciences

Approved: _____
John Pelesko, Ph.D.
Dean of the College of Arts and Sciences

Approved: _____
Douglas J. Doren, Ph.D.
Interim Vice Provost for Graduate and Professional Education and Dean
of the Graduate College

ACKNOWLEDGMENTS

I want to begin by thanking my advisor, Dr. Donna Woulfe, without whom, my master's thesis would not be possible. I cannot begin to express my gratitude for her unwavering support and dedication to both my personal and professional growth over the past three years. Readily available to help with all questions ranging from the simplest protocol confirmations to larger troubleshooting issues and gaining a deeper understanding of the conceptual underpinnings of my project, she always greeted me with patience and understanding. She believed in me through moments where I found it impossible to believe in myself.

I also want to thank my committee members, Dr. Erica Selva and Dr. Jeffrey Caplan, for their valuable feedback and support even outside of our scheduled meetings. Despite their demanding schedules, they were highly invested in my success and readily offered assistance when I needed it most.

A big “thank you” to our past lab members, Fawziya Barnawi and Conroy Field. Part of the reason I fell in love with this lab was due to their warm personalities, kindness, and willingness to help. Their patience through training allowed me to learn from mistakes and gave me the confidence to ultimately work independently. I genuinely miss all the fun times we have had, i.e. lab lunches, movie nights, and our summer trip to the aquarium.

Thank you to the University of Delaware and the Department of Biological Sciences for accepting me into this prestigious program and providing all the resources necessary for me to succeed. I want to take a moment to thank Betty

Cowgill for keeping me on track in the program with friendly reminders and a helping hand. Thank you to the faculty for guidance both within and outside of research. The opportunity to TA has been one of the most memorable and rewarding experiences of my graduate career. I personally want to thank Dr. Mahaffy, Dr. Ketcham, and Dr. Walsh for making it possible.

Thank you to the Delaware Biotechnology Institute, particularly the Bioimaging Center for the use of instrumentation, critical for the completion of my project. I also want to thank the staff both past and present, including Michael Moore, Dr. Le Marchand, and in particular, Dr. Caplan for getting me started with fluorescence correlation spectroscopy and providing training and continuous support in using the LSM880 confocal microscope.

I would like to thank my parents, Annmarie and Phil Giordano, who have encouraged me throughout my life to pursue my passions and never give up. I've dreamed of becoming a scientist since middle school and cannot believe I have finally made it to this stage. Thank you for putting up with my quirkiness, independence, and unconventional ways of having fun in my youth (including, but not limited to, the mess I made extracting strawberry DNA at a hosted sleepover party-perhaps it has finally paid off?).

Lastly, I would like to thank the remainder of my family and friends who stood by me through this journey. Although I had been distant in both miles and communication, they have shown me nothing but support and understanding. Knowing that I wasn't alone and isolated as originally thought, gave me the strength to push forward through the challenges of research. Thank you to all, including those not specifically mentioned here, who have been part of my graduate education!

TABLE OF CONTENTS

LIST OF FIGURES	viii
ABSTRACT	xiii

Chapter

1	INTRODUCTION	1
1.1	GPCR Structure and Activation	1
1.2	Signal Termination, Desensitization, and G-Protein-Independent Signaling.....	4
1.3	GPCR Families	6
1.4	Oligomeric Tendencies of GPCRs	7
1.5	Techniques to Investigate GPCR Dimerization	10
1.6	Overview of the Role of Platelets in Hemostasis and Thrombosis	14
1.7	Platelet Purinergic and Protease-Activated Receptors	15
1.8	Dimerization of Platelet GPCRs.....	17
1.9	Naturally-Occurring Mutant Variants of P2Y12	20
2	MATERIALS AND METHODS	26
2.1	Cell Culture	26
2.2	Akt Activation Experiments	26
2.2.1	Plasmid Constructs	26
2.2.2	Generation of Stable Cell Lines	27
2.2.3	Preparation of Cells and Western Blotting.....	27
2.2.4	Statistical Analysis	28
2.3	Fluorescence Correlation Spectroscopy (FCS) and Photon Counting Histogram (PCH) Experiments	28
2.3.1	Plasmid Constructs	28
2.3.2	Cell Culture and Transfection	29
2.3.2.1	Homomeric Interactions of Wild-Type P2Y12 and Mutant Variants, R265W and D121N	29

2.3.2.2	Heteromeric Interactions of P2Y12 Mutant Variant R265W with PAR4.....	29
2.3.3	System Settings for FCS and PCH Analysis	30
2.3.4	Pinhole Alignment.....	31
2.3.5	Statistical Analysis	31
2.4	G α i-Coupling of P2Y12 Receptor	32
2.4.1	Plasmid Constructs	32
2.4.2	GloSensor cAMP Assay	33
2.4.3	Statistical Analysis	34
3	RESULTS.....	35
3.1	Activation of Akt by P2Y12 Mutant Variants.....	35
3.1.1	Background.....	35
3.1.2	P2Y12 Mutant Variants R265W and D121N Have Increased Constitutive Activity in Phosphorylation of Akt.....	37
3.2	Structural Analysis of P2Y12 Mutant Variants: Investigating Homo- and Heterodimerization	40
3.2.1	Background.....	40
3.2.2	P2Y12 Mutant Variant R265W, but Not D121N, Forms Increased Homodimers	41
3.2.3	P2Y12 Mutant Variant R265W Heterodimerization with PAR4	44
3.3	G α i Coupling of P2Y12 Mutant Variants R265W and D121N.....	46
3.3.1	Background.....	46
3.3.2	Mutant Variants R265W and D121N are Able to Couple to G α i in a Manner Comparable to Wild-Type P2Y12 in HEK293T Cells	48
4	DISCUSSION AND FUTURE DIRECTIONS.....	51
4.1	P2Y12 Mutant Variant R265W	51
4.2	P2Y12 Mutant Variant D121N.....	55
4.3	Summary of Conclusions	59
4.4	Future Directions	61
4.4.1	Investigate Dimeric Potential of P2Y12 Mutant Variant D121N with Wild-Type Receptor	61

4.4.2	Determine the Ability of P2Y12 Mutant Variants to Heterodimerize to PAR4 Relative to That of WT P2Y12.....	62
4.4.3	Arrestin-2 Recruitment to P2Y12 Mutant Variants and PAR4...	62
REFERENCES	64

LIST OF FIGURES

- Figure 1: **Summary of canonical G-protein-coupled receptor signaling.** GPCRs are associated with heterotrimeric G proteins, composed of an alpha (α), beta (β), and gamma (γ) subunit, associated with GDP when the receptor is in an inactive state. Upon agonist binding, the receptor undergoes a conformational change inducing the exchange of GDP for GTP on the α subunit. Subsequently, the α subunit dissociates from the receptor and from $\beta\gamma$. Both the α and $\beta\gamma$ subunits participate in intracellular signaling events (adapted from Li *et al* 2002). 2
- Figure 2: **Modulation of receptor-mediated signaling.** GPCRs may exhibit constitutive activity that can be altered by a variety of compounds which fall into four main categories: full agonists, partial agonists, neutral antagonists, and inverse agonists. Each stabilizes the receptor into different conformational states of varying degrees of activity (adapted from Wacker *et al* 2017). 4
- Figure 3: **Overview of Fluorescence Correlation Spectroscopy (FCS).** **A.** General set-up of a confocal microscope featuring an objective lens with high numerical aperture. A laser is used to focus light on a sample at a particular excitation wavelength. Light emitted from fluorescent species pass through a pinhole before reaching the detector. **B.** Fluorescently-tagged proteins are free to diffuse through the small illuminated volume (confocal volume), resulting in fluctuations in fluorescence intensity as these species pass into the confocal volume and become excited by the laser. **C.** These changes in intensity over time are recorded and used for further analysis such as autocorrelation and photon counting histogram (PCH) (adapted from Kilpatrick & Hill 2016). 12

Figure 4: **Autocorrelation analysis and photon counting histogram.**
 Fluorescence correlation spectroscopy (FCS) recordings can be used for autocorrelation analysis (A) (adapted from Bacia *et al* 2006) and photon counting histogram (PCH) (B) (adapted from Youker & Teng 2014). Autocorrelation curves provide information about the number and diffusion rates of fluorescent particles in the confocal volume, while PCH shows the number of photon counts per “bin” of the total FCS observation period. PCH is used to determine the average oligomer size of fluorescently-tagged particles..... 14

Figure 5: **P2Y12 exists predominately as a monomer on the membrane of live cells.** HEK293T cells were transiently transfected with CD86-GFP (monomeric control), CD86-GFPGFP (dimeric control), and WT P2Y12-GFP. Molecular brightness was determined at 36 hours post-transfection via FCS and one-component PCH analysis. Error bars represent standard deviation. ** $p < 0.001$, student’s t-test. There was no significant difference in molecular brightness between CD86-GFP and WT P2Y12-GFP ($p=0.699$, student’s t-test) (adapted from Barnawi 2017). 19

Figure 6: **Snake plot of the human purinergic platelet receptor, P2Y12.** P2Y12 is a class A G-protein-coupled receptor (GPCR) expressed mainly on platelets and is important for their aggregation. Human P2Y12 is made up of 342 amino acids with the N-terminus oriented extracellularly and the C-terminus, cytosolically. Here, conserved transmembrane (TM) residues are circled in red, while two N-linked glycosylation sites found to be important for signal transduction are shown in yellow. Amino acids in blue represent documented positions that have been mutated in patients with a bleeding phenotype (adapted from Cunningham *et al* 2013). 21

Figure 7: **P2Y12 expression in HEK293T cells stably expressing WT P2Y12 or P2Y12 mutant variants R256Q or R265W.** HEK293T cells stably expressing Flag-tagged WT P2Y12, or one of two P2Y12 mutant variants, R256Q or R265W, were grown to 70% confluency, serum starved for 12 hours, and lysed. Untransfected HEK293T cells were lysed and used as a negative control. Lysates were run on 10% SDS-polyacrylamide gel and immunoblotted for P2Y12 (1:100, Santa Cruz Biotechnologies)..... 22

- Figure 8: **P2Y12 mutant variants R265W and R256Q form a higher proportion of homodimers than WT P2Y12.** HEK293T cells were transiently transfected with GFP-tagged WT P2Y12, or mutant variants R265W or R256Q. Molecular brightness was determined at 36 hours post-transfection via FCS and one-component PCH analysis. Error bars represent standard deviation. * $p < 0.01$, student's t-test (adapted from Barnawi 2017). 23
- Figure 9: **P2Y12 mutant variant R256Q failed to activate G α i.** HEK293T cells were transiently co-transfected with pGloSensor-20F cAMP plasmid and pcDNA (mock), WT P2Y12, or P2Y12R256Q. Cells were either left untreated, or treated with forskolin alone (10 μ M) or in the presence of ADP (10 μ M), and the accumulation of cAMP was measured by luminescence (RLU). Presented is the mean +/- SD of three independent experiments, *** $p < 0.0001$, ANOVA (adapted from Barnawi 2017). 23
- Figure 10: **Schematic of GloSensor Technology.** pGloSensor-20F cAMP plasmid (Promega) allows for heterologous expression of a modified form of the firefly (*Photinus pyralis*) luciferase containing a binding site for cAMP. Analyte binding leads to a conformational change that promotes an increase in luminescence activity. Therefore, the magnitude of this increased light output is directly proportional to the amount of cAMP present in live cells (adapted from Fan *et al.* 2008). .. 32
- Figure 11: **Confirmation of P2Y12 and PAR4 expression in HEK293T stable cell lines.** HEK293T cells were co-transfected with HA-PAR4, and either WT Flag-P2Y12, Flag-P2Y12R265W, or Flag-P2Y12D121N. Cells were selected in hygromycin (400 μ g/mL) and geneticin (1000 μ g/mL) for 3 weeks, and then maintained in lower concentrations of hygromycin (200 μ g/mL) and geneticin (500 μ g/mL). Stables were grown to 70% confluency in 6-well plates, serum-starved for 12 hours, lysed, and run on a 10% SDS-polyacrylamide gel. An untransfected HEK293T cell lysate was run as a negative control. Immunoblots were probed for **(A)** P2Y12 (1:100, Santa Cruz Biotechnology) or **(B)** PAR4 (1:750, Cell Signaling Technologies), and developed using a ChemiDoc imaging system (Bio-Rad)..... 37

- Figure 12: **Mutant variants of P2Y12, R265W and D121N, have increased constitutive Akt phosphorylation.** Stable HEK293T cell lines, co-expressing PAR4 and WT P2Y12 or one of two P2Y12 mutant variants, R265W or D121N, were grown to 70% confluency and serum starved for 12 hours. Cells were left untreated or treated with ADP (10 μ M) for 10 minutes at 37°C. Presented is the quantification of p-Akt normalized to total Akt +/- SEM from 5 independent experiments, ** p<0.01 unpaired t-test (A). A representative blot using antibodies against phospho-Akt(S473) (1:500, Cell Signaling Technologies) and total Akt (1:1500, Cell Signaling Technologies), is shown (B). 39
- Figure 13: **Live cell imaging of HEK293T cells expressing P2Y12 eGFP constructs.** HEK293T cells were transiently transfected with eGFP-tagged WT P2Y12 (A), or P2Y12 mutant variants R265W (B) or D121N (C) and imaged by confocal microscopy (Zeiss LSM880) at 36-hours using a 40x water-immersion lens. Zen Black 2.1 software (Zeiss) was used to process the fluorescent and DIC merged images as shown. Yellow scale bar, 20 μ m. 42
- Figure 14: **P2Y12 mutant variant R265W has tendency towards increased homodimerization.** HEK293T cells were transiently transfected with CD86-GFP (as a monomeric control), CD86-GFPGFP (as a dimeric control), P2Y12-GFP or P2Y12R265W-GFP and analyzed by FCS and PCH at 36 hours post-transfection. Molecular brightness was measured to determine the oligomeric state of the receptors, which was normalized to the monomeric control (CD86-GFP, set to 1). Presented is the mean of four independent experiments +/- SEM; p = 0.07, paired student's t-test. 43
- Figure 15: **P2Y12 mutant variant D121N does not form increased homodimers relative to the WT receptor.** HEK293T cells were transiently transfected with CD86-GFP (as a monomeric control), CD86-GFPGFP (as a dimeric control), P2Y12-GFP or P2Y12D121N-GFP and analyzed by FCS and PCH at 36 hours post-transfection. Molecular brightness was measured to determine the oligomeric state of the receptors, which was normalized to the monomeric control (CD86-GFP, set to 1). Presented is the mean of two independent experiments +/- SEM; n.s., not significant, paired student's t-test 44

Figure 16: **P2Y12 mutant variant R265W may heterodimerize with PAR4.** HEK293T cells were transiently transfected with CD86-GFP (monomeric control), CD86-GFPGFP (dimeric control), P2Y12-GFP, and P2Y12 mutant variant R265W-GFP, or co-transfected with P2Y12R265W-GFP and HA-PAR4 in a ratio of 1:1, 1:4, and 1:16. Cells were analyzed by FCS and PCH at 36 hours post transfection. Molecular brightness (in cpsm, counts per second per molecule) was measured to determine the oligomeric state of the receptors. Presented is the mean of 3 to 4 cells +/- SEM from a single experiment. 46

Figure 17: **P2Y12 mutant variants R265W and D121N do not show Gai coupling defect in a heterologous expression system.** HEK293T cells were transiently co-transfected with pGloSensor-20F cAMP plasmid (20F) along with pcDNA (mock-N=4), P2Y12-GFP (N=4), P2Y12R265W-GFP (N=5), or P2Y12D121N-GFP (N=3). At 36-72 hours post-transfection, cells were lifted, equilibrated in cAMP reagent, and transferred to a 96-well plate. Cells were left untreated or treated with 0.4µM forskolin with or without 0.4µM ADP. Luminescence was measured to determine the relative levels of cAMP present in the cells. Data was normalized to the percentage of forskolin-induced cAMP activity. Error bars represent SEM. 49

ABSTRACT

G-protein-coupled receptors (GPCRs) constitute the largest family of receptors in humans, responding to a wide range of stimuli, and responsible for nearly every physiological process. Their pharmacological significance is unprecedented with around a third of FDA-approved drugs targeting these receptors (Sriram & Insel 2018).

In platelets, GPCRs play a vital role in their activation and aggregation. Platelets are anucleate cells that contribute to both protective hemostasis and pathophysiological thrombosis. Humans express two purinergic receptors, P2Y1 and P2Y12, and two protease-activated receptors, PAR1 and PAR4, on the plasma membrane of platelets (Abbracchio *et al* 2006; Coughlin 2005). P2Y12 is of particular significance as it is the target of clinically effective anti-thrombotic drugs and is the focus of this study.

While P2Y1 and PAR1 are required for the initiation of platelet activation, P2Y12 and PAR4 are important for stable responsiveness. PAR4 is activated by thrombin, the most potent platelet activator, and signals through G α q which initiates intracellular events leading to the release of dense granules (Coughlin 2005). Dense granules release a variety of signaling molecules extracellularly including ADP, which is the agonist for P2Y12. P2Y12 is coupled to G α i and therefore decreases cAMP levels in the cell (Abbracchio *et al* 2006). Both PAR4 and P2Y12 can independently activate Akt, but synergy between the two receptors is required for maximal Akt activation for stable thrombi *in vivo* (Li *et al* 2011).

Our understanding of how GPCRs operate has changed in recent years. Historically thought to exist as monomeric entities transducing signals through a single G protein and adopting only one of two conformational states (on or off), GPCRs are now understood to form dimers (Gurevich & Gurevich 2008), couple to more than one G protein (Wenzel-Seifert & Seifert 2000), and adopt multiple agonist-dependent conformations of varying levels of activity (Swaminath *et al* 2005).

Increasing evidence supports that dimerization plays a pivotal role in normal cell signaling and further diversifies receptor responses. While it has become clear that class C GPCRs form obligate homo- and heterodimers, the characterization of class A oligomers in both their size and function, remains elusive (Gurevich & Gurevich 2008). Our lab has shown that class A GPCRs, P2Y₁₂ and PAR4 directly and specifically associate with each other in a functionally relevant manner (Khan *et al* 2014). Disrupting their heterodimerization significantly decreased phospho-Akt levels when the receptors were co-expressed heterologously in HEK293T cells.

Recently, our lab became interested in naturally-occurring mutant variants of P2Y₁₂ that have been identified in two patients found to have platelet aggregation defects. The first patient had a lifelong history of bleeding and was found to be compound heterozygous for two mutant variants of P2Y₁₂: R256Q and R265W. These receptors have been shown to have normal surface expression and agonist binding but have a G α i defect in platelets (Cattaneo *et al* 2003). Given that the mutations are not present cytosolically where we would expect direct physical association with the G protein, these mutations may affect coupling through altering receptor structure. The second patient was heterozygous for a mutation resulting in an aspartic acid to asparagine substitution at amino acid position 121 of P2Y₁₂ (D121N)

(Kostyak *et al* 2018). It is surprising that isolated platelets from this subject are virtually unresponsive to agonist ADP, given that the subject is heterozygous for the D121N mutation. It is expected that this individual would express a wild type P2Y₁₂ receptor encoded by the remaining gene copy and therefore be able to functionally compensate. This mutation is located in the highly conserved DRY motif of GPCRs which is thought to be important for G protein coupling, receptor conformational states, and trafficking (Nygaard *et al* 2009). This mutation may structurally alter the receptor in a manner resulting in its apparent dominant negative phenotype.

Interestingly, the crystal structure of P2Y₁₂ packed as a dimer (Zhang *et al* 2014b), and treatment of cells with the active metabolite of a P2Y₁₂ antagonist decreased the proportion of apparent P2Y₁₂ oligomers resolved on SDS-PAGE (running as higher-than-expected molecular weight bands on immunoblots) (Savi *et al* 2006). This is suggestive that the functional unit of P2Y₁₂ is at least a dimer, if not a higher-ordered oligomer. The aforementioned P2Y₁₂ mutant variants may have an altered ability to homodimerize or heterodimerize with PAR4, in-turn affecting their function and providing an explanation for the observed phenotype in patients.

Using fluorescence correlation spectroscopy (FCS), my lab has found the predominant species of P2Y₁₂ to be a monomer on the plasma membrane of live HEK293T cells for the first time. Interestingly, we found that P2Y₁₂ mutant variants R256Q and R265W have a higher tendency to homodimerize compared to the wild-type receptor. Furthermore, P2Y₁₂R256Q, when expressed in isolation was unable to reduce forskolin-induced cAMP activity, suggesting an inability to couple G_{ai} (Barnawi 2017). Since P2Y₁₂R265W was found to exhibit a more severe homodimerization defect relative to P2Y₁₂R256Q, I decided to further investigate

potential structural and functional properties of this receptor. Additionally, I aimed to characterize the functional deficits and dimerization potential of P2Y12D121N to begin to understand the potential dominant-negative function of this mutation in platelet aggregation.

Here, I found that both P2Y12 mutant variants R265W and D121N exhibit constitutive activity in phosphorylation of Akt, which may be explained through cooperation with PAR4. Consistent with this hypothesis, I found that P2Y12R265W may physically associate with PAR4. The tendency of P2Y12R265W, relative to WT P2Y12, to heterodimerize with PAR4 as well as P2Y12D121N/PAR4 interactions, have yet to be investigated. Additionally, the DRY motif has been found to participate in interactions that maintain GPCRs in an inactive state. A charge-neutral mutation of aspartic acid to asparagine may induce constitutive activity.

Through FCS, I confirmed previous findings from my lab that P2Y12R265W forms increased homodimers relative to wild type receptor, whereas P2Y12D121N does not homodimerize. It has yet to be determined whether P2Y12D121N may dimerize with the wild-type receptor. Finally, I show that neither P2Y12R265W or P2Y12D121N have a defect in *G_{ai}* coupling, as revealed through a bioluminescence-based cAMP assay in live cells.

It was surprising to us that P2Y12R265W exhibited no defect in forskolin-induced cAMP inhibition, as we expected its increased homodimerization would preclude either activation of G protein or its association with the receptor; however, this further highlights the complex relationship between GPCR structure and signaling. Our results are suggestive that constitutive activity of these P2Y12 mutant variants promotes agonist-independent desensitization. This would severely reduce

ADP-dependent platelet aggregation as observed in the compound heterozygous P2Y₁₂-R256Q/R265W patient and the P2Y₁₂D121N heterozygous individual.

Chapter 1

INTRODUCTION

1.1 GPCR Structure and Activation

G protein-coupled receptors (GPCRs) make up the largest and most diverse family of plasma membrane receptors, transducing signals from a wide range of stimuli including neurotransmitters, hormones, small molecules, and photons. Despite their structural and functional diversity, all GPCRs have a common topology consisting of seven alpha helical transmembrane domains with alternating intracellular and extracellular loops. The N terminus is oriented extracellularly and the C terminus, cytosolically (Kroeze *et al* 2003).

GPCRs are coupled to heterotrimeric G proteins, which are composed of alpha, beta and gamma subunits. They are classified based upon the identity of the alpha subunit, which can be categorized into one of four different groups: alpha s, alpha i, alpha q, and alpha 12/13. Each of these subgroups induces differential signaling cascades via interaction with distinct effectors (Hilger *et al* 2018). Alpha s characteristically induces activation of adenylyl cyclase, alpha i induces inhibition of adenylyl cyclase, alpha q induces activation of phospholipase C, and alpha 12/13 induces activation of small GTPases, with consequent actin rearrangement (Penn & Benovic 2008).

Canonical signaling of GPCRs involves a conformational change of the receptor after ligand binding to its extracellular surface. This conformational change in turn induces exchange of GDP for GTP on the alpha subunit of the coupled

heterotrimeric G protein, which can then activate the downstream effector (Figure 1). This simple model involves a single receptor which then activates one G protein. While there is evidence that a 1:1 stoichiometry of receptor: G protein exists (Gao *et al* 2017; Wenzel-Seifert & Seifert 2000), today, it is thought that this model is not sufficient to reflect the highly dynamic nature of GPCRs. Different GPCRs may exhibit different ligand-dependent conformations and levels of activity (Swaminath *et al*, 2005), couple to more than one G protein subtype (Wenzel-Seifert & Seifert 2000), signal through G-protein independent pathways (Barthet *et al* 2009), and interact with other GPCRs (Khan *et al* 2014; Liang *et al* 2003; Tabor *et al* 2016).

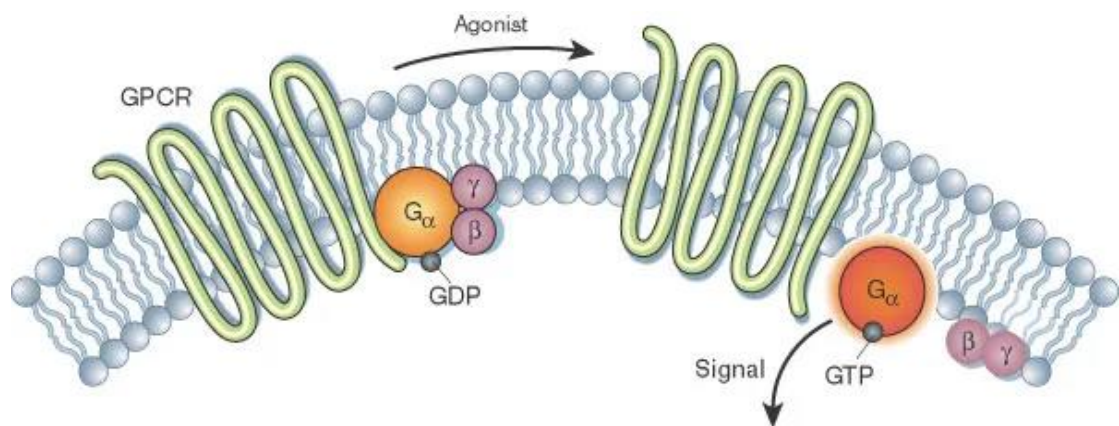


Figure 1: **Summary of canonical G-protein-coupled receptor signaling.** GPCRs are associated with heterotrimeric G proteins, composed of an alpha (α), beta (β), and gamma (γ) subunit, associated with GDP when the receptor is in an inactive state. Upon agonist binding, the receptor undergoes a conformational change inducing the exchange of GDP for GTP on the α subunit. Subsequently, the α subunit dissociates from the receptor and from $\beta\gamma$. Both the α and $\beta\gamma$ subunits participate in intracellular signaling events (adapted from Li *et al* 2002).

A particular GPCR may have multiple agonists that can bind to the receptor and modulate its function. Some receptors bind to a diverse complement of full or partial agonists, as well as inverse agonists and antagonists. The binding of these molecules can induce different conformations of the receptor that allow for multiple levels of activity, rather than acting as a simple bimodal switch. (Figure 2; Rosenbaum *et al* 2009). For example, the beta2 adrenergic receptor (β 2AR) can interact with the aromatic ring of two different agonists via binding to different regions of the receptor and in turn induces different receptor conformations. Specifically, the structure of the catecholamine full agonist isoproterenol and non-catechol partial agonist salbutamol are very similar; however, they do not compete with each other for binding. Due to the differences in interactions with the receptor, they induce different conformational changes in the receptor, allowing the receptor to be more (full agonist) or less (partial agonist) activated (Swaminath *et al* 2005).

Structurally, an area of the receptor termed the “toggle switch” appears to be important in full activation of GPCR. The toggle switch refers to the reorganization of regions of TM6 bringing key amino acids in close proximity of each other to interact. Interestingly, some β 2AR agonists only partially increase receptor activity likely due to their inability to activate this switch (Swaminath *et al* 2005).

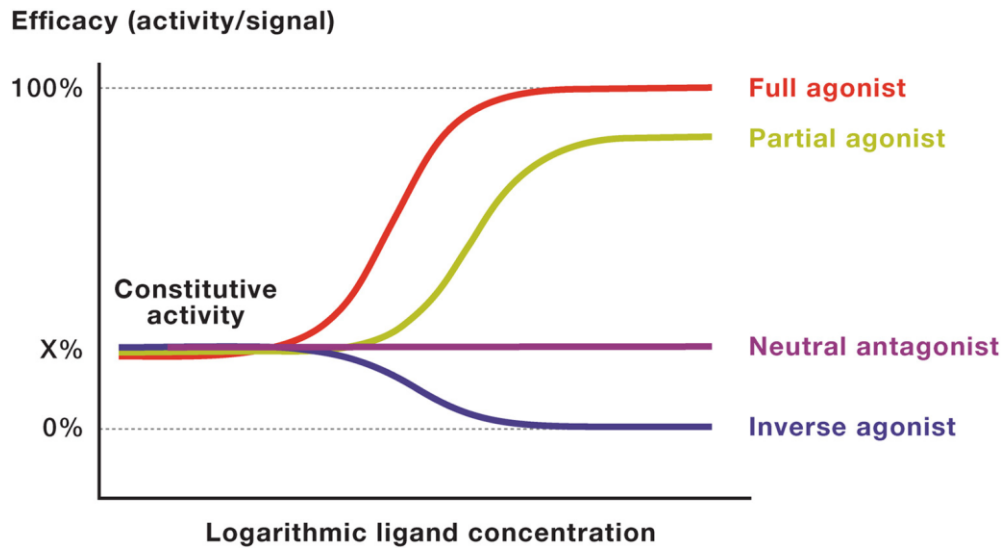


Figure 2: **Modulation of receptor-mediated signaling.** GPCRs may exhibit constitutive activity that can be altered by a variety of compounds which fall into four main categories: full agonists, partial agonists, neutral antagonists, and inverse agonists. Each stabilizes the receptor into different conformational states of varying degrees of activity (adapted from Wacker *et al* 2017).

1.2 Signal Termination, Desensitization, and G-Protein-Independent Signaling

GPCRs signaling is tightly regulated. After agonist binding, intracellular responses peak within milliseconds to minutes and then rapidly decline after a brief plateau (Rajagopal & Shenoy 2017). Signaling can be terminated by dissociation of an agonist from the receptor which subsequently destabilizes the active conformation. Additionally, the heterotrimeric G protein becomes inactivated through hydrolysis of GTP to GDP on the alpha subunit by a combination of its intrinsic “GTPase-activating protein” (GAP) activity and interaction with “regulator of G protein signaling” (RGS) proteins (Siderovski & Willard 2005). However, GPCR signaling can still be negatively regulated even with bound agonist. Reducing the response of prolonged

stimulation and preventing subsequent agonist-dependent activation is referred to as desensitization, which is critical for normal cell function (Rajagopal & Shenoy 2017).

The process of desensitization involves phosphorylation of GPCRs on specific cytosolic domains and the binding of arrestins with high affinity which prevents further activation of G protein by steric hinderance and promotes internalization (Luttrell & Gesty-Palmer 2010; Rajagopal & Shenoy 2017). There are two main types of desensitization: homologous and heterologous. Homologous desensitization involves the loss of agonist-dependent responsiveness of a particular GPCR subtype. Heterologous desensitization refers to a more generalized loss of response initiated by agonist-dependent GPCR signaling, but potentially effecting other GPCR subtypes not bound to agonist. An example would be phosphorylation of specific intracellular serine/threonine residues of the receptor by PKA which is activated by GPCR second messengers. While this mechanism is not specific for agonist-bound GPCRs, it acts as a negative feedback loop for those that are agonist-bound and actively participating in this signaling pathway (Kelly *et al* 2007).

GPCR regulatory kinases (GRKs) specifically phosphorylate agonist-bound GPCRs in homologous desensitization. This promotes the binding of arrestins and internalization of the receptor through clathrin-mediated endocytosis (Ferguson 2007). Arrestins can also act as multiprotein scaffolds for mediators of other signaling pathways, such as the MAP kinase and PI3K/Akt cascade (DeWire *et al* 2007; Irannejad & Zastrow 2014). In this way, GPCRs can participate in signaling that is independent of activated G-proteins (Ferguson 2007). Following dephosphorylation of the cytosolic domains of GPCRs, they can either be recycled to the plasma membrane

(re-sensitization) or trafficked to lysosomes for degradation (Irannejad & Zastrow 2014).

1.3 GPCR Families

GPCRs can be grouped into different classes according to structural homology. Class A (rhodopsin-like), class B (secretin-like), class C (glutamate), and class F (frizzled) are expressed in humans. Class A is the largest of these classes consisting of over 700 receptors (Venkatakrishnan *et al* 2014).

In general, intracellular regions are more conserved across GPCR classes than extracellular regions. It is suggested this is due to the limited number of G proteins that can couple to the receptor (alpha s, i, q, and 12/13) as opposed to the diverse number and type of ligands that can bind to the extracellular surface. Classes B, C and F have long structured extracellular domains important for ligand binding (Venkatakrishnan *et al* 2014).

For class B GPCRs, agonists bind to the extracellular domain (ECD) which confirms specificity, and then to a “binding pocket” formed by the seven transmembrane regions arranged to form a bundle, known as the 7TM or heptahelical domain (HD), to activate the receptor. Class C function as obligate homo- or heterodimers. Like class B, they have an ECD, but it is much larger and is the orthosteric binding site for ligands, as ligands do not interact with a pocket in the 7TM domain. The ECD in class C forms a venus fly trap (VFT) domain that is very highly conserved and can be in an open or closed conformation. A few class A GPCRs have a large extracellular domain to bind ligand, but most orthosteric sites lie exclusively within the 7TM domain. While this is a shared feature among class A receptors, there

is huge diversity in the architecture and access of these binding pockets among different receptors to accommodate the diverse range of ligands (Lee *et al* 2015).

1.4 Oligomeric Tendencies of GPCRs

Historically, GPCRs were thought to be monomeric, but increasing evidence has pointed to functional GPCR dimers and higher-order oligomers. It is currently well-documented that class C GPCRs exist as obligate dimers. In contrast, the functional unit of the receptor and role of oligomerization are not fully understood for members of the largest class A (Gurevich & Gurevich 2008), which is of particular interest in this study.

Both homodimers (calcium sensing receptor and metabotropic glutamate receptors (mGluRs)) and heterodimers (GABA_B and sweet and umami taste receptors) have been documented for class C GPCRs. The best studied heterodimer is the GABA_B receptor (Milligan 2008).

By the late 1990s, two splice variants of GABA_B had been cloned: GABA_BR1a and GABA_BR1b. When either or both splice variants were expressed heterologously, they were not functional as determined by measuring cAMP production and activation states of downstream ion channels. Furthermore, differences in binding ability of GABA_B receptors in native cells was observed, suggesting the existence of multiple subtypes. A new subtype of GABA_B, termed GABA_BR2, was found having 35% identity to GABA_BR1a/b. This subtype does not bind agonist with measurable potency (Kaupmann *et al* 1998), but can associate with GABA_BR1a/b through a coiled-coil domain in the C terminal tail (White *et al* 1998).

It was proposed that GABA_BR2 was required for GABA_BR1 trafficking to the plasma membrane and that the heterodimer was the functional unit of the receptor.

Flow cytometry studies revealed that GABA_BR1a/b could only be detected in permeabilized HEK293T cells when transfected alone but expressed on the plasma membrane when co-transfected with GABA_BR2, and *in situ* hybridization revealed colocalization of the two receptor subtypes in the hippocampus and cortex of the human brain (White *et al* 1998). Expression of both GABA_BR1a/b and GABA_BR2 were required for activation of the Kir3 K⁺ channel (Kaupmann *et al* 1998). Further studies demonstrated that one protomer binds ligand in VFT domain while the other couples G protein.

Evidence for class C GPCR dimers led to the question as to whether class A could dimerize as well. Class C receptors could be activated by allosteric ligand binding to the heptahelical transmembrane domain in a similar fashion as the orthosteric ligands bind class A. Additionally the cytoplasmic surface area of class A receptors such as rhodopsin are small relative to heterotrimeric G proteins and arrestins that bind activated GPCRs, suggesting that a dimer could bind these molecules (Gurevich & Gurevich 2008). Although the crystal structure of monomeric beta2 adrenergic receptor (β 2AR) revealed physical association with only the alpha subunit of G α s, it was proposed that the $\beta\gamma$ subunits may associate with a second protomer in a dimeric unit for a 2:1 stoichiometry of receptor to G-protein (Rasmussen *et al* 2011).

While there have been documented cases of dimerization and oligomerization in class A GPCRs such as rhodopsin, β 2AR, and dopamine D2 receptor (D2R), the function of these clusters remains unclear and highly debated. Dimers may be stable or transient, and either enhance or impede signaling (Gurevich & Gurevich 2008).

Although β 2AR was found to form constitutive homodimers via bioluminescence resonance energy transfer (BRET) (Angers *et al* 2000), a monomer is sufficient to activate G protein (Whorton *et al* 2007). Furthermore, while rhodopsin dimers were found in native tissue (Liang *et al* 2003), evidence suggests that dimerization may reduce signaling. Researchers generated nanodiscs containing either one or two rhodopsin molecules. Using a GTP γ S exchange assay, they found that the activity of rhodopsin on nanodiscs containing two molecules was half that of monomeric rhodopsin. It is suggestive that when either two rhodopsin molecules are in close proximity, or in a dimeric state, only one is available to interact with its G protein, transducin (Bayburt *et al* 2007).

In contrast, another study found that rhodopsin oligomers were actually faster than monomers in activating transducin (Jastrzebska *et al* 2006). Additionally, D2R dimers and monomers exist in equilibrium but the proportion of dimers increases in the presence of agonist, suggesting that homodimerization is important for receptor activation and efficient signaling (Tabor *et al* 2016). Another study not only identified TM4 as the interface for homodimerization in D2R, but found that the degree of cross linking of key cysteine residues between two protomers at this interface increased in the presence of agonist and promoted the active-state of the receptor (Guo *et al* 2005).

Dimerization may also play a role in different “life-cycle” stages of a receptor such as maturation, trafficking, and internalization. β 2AR dimerization-defective mutants had reduced targeting to the plasma membrane by over 50% compared to the wild-type receptor which normally forms homodimers in the ER (Salahpour *et al* 2004). While β 2AR homodimers appear to be critical for mediating their own surface expression, β 2AR heterodimerization significantly enhanced mouse 71 olfactory

receptor expression on the plasma membrane of HEK293T cells (Hague *et al* 2004). Internalization of β 2AR and subsequent phosphorylation of ERK1/2 following treatment with the nonselective β -adrenergic agonist isoproterenol was significantly reduced when co-expressed with β 1AR. Since the receptors were found to co-immunoprecipitate, it was proposed that this alteration to β 2AR signaling observed when expressed in isolation, was due to heterodimerization with β 1AR (Lavoie *et al* 2002).

1.5 Techniques to Investigate GPCR Dimerization

GPCR interactions classically have been investigated using co-immunoprecipitation, resonance energy transfer (RET), and bimolecular fluorescence complementation (BiFC). While these techniques provide valuable insights, they are limited in a few key respects. Co-immunoprecipitation requires disruption of the plasma membrane resulting in detected interactions that may not reflect those present in living cells. Resonance energy transfer techniques and BiFC are performed in live cells but lack the spatial resolution to separately investigate fluorescently tagged moieties in specific regions of a single cell. (Kilpatrick & Hill 2016; Scarselli *et al* 2015). RET techniques require energy donor/acceptor pairs of either two fluorophores (Förster RET) or one fluorophore and luciferase (bioluminescence RET), that are each individually fused to proteins of interest. The acceptor becomes excited when in close proximity to the donor, and consequently emits light at a unique wavelength. (Lohse *et al* 2012).

BiFC is a technique by which a fluorophore is separated into two non-fluorescent fragments: N-terminal and C-terminal end, each fused to candidate proteins. If the proteins interact, then the two fragments will re-combine into the

whole functional fluorophore (Kerppola 2008). This has the advantage over RET techniques in that it measures direct protein-protein interactions rather than relying on the proximity of donor-acceptor molecules (Lai & Chiang 2016). However, BiFC is irreversible and therefore cannot detect dynamic protein interactions (Kerppola 2008).

Fluorescence correlation spectroscopy (FCS) has an advantage over these traditional methods in that it can measure the spatial and temporal interactions of single fluorescently-tagged molecules on individual live cells (Kilpatrick and Hill 2016). Additionally, proteins can be studied at or near physiological concentrations (Vischer *et al* 2015). FCS has been used to study diffusion dynamics of gold-nanospheres in cells for biomedical applications (Liu *et al* 2018), protein-protein interactions including those between GPCRs (Herrick-Davis *et al* 2012; Herrick-Davis *et al* 2013; Herrick-Davis *et al* 2015; Petersen *et al* 2017), and ligand-receptor complexes (Briddon & Hill 2007). My lab uses FCS to study the dimerization potential of the purinergic platelet receptor, P2Y₁₂, and naturally-occurring P2Y₁₂ mutant variants, in real time, on the plasma membrane of live HEK293T cells.

FCS is a confocal technique that requires an objective lens with high numerical aperture. The laser illuminates a small Gaussian-shaped detection volume (confocal volume) of 0.25–0.5 fl (Briddon & Hill 2007) in the sample, created by a pinhole through which light must pass before reaching the detector. The fluorescently-tagged molecules diffuse in and out of the confocal volume and emit light as they are excited by the laser. This creates fluctuations in fluorescent intensity over time which is captured by the microscope and can be further analyzed with imaging software (Figure 3; Kilpatrick & Hill 2016).

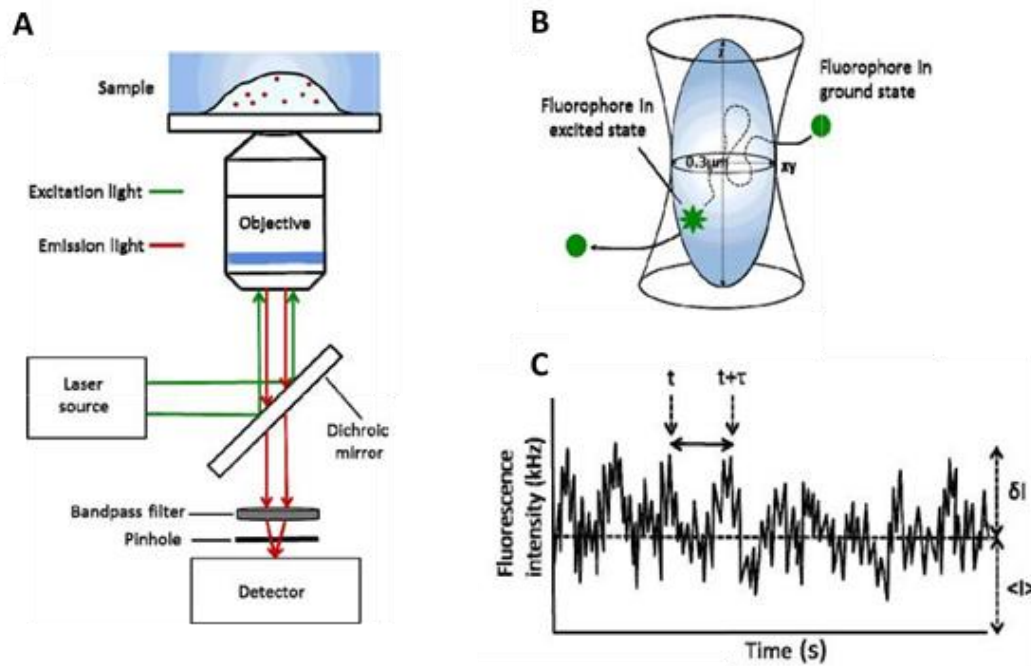


Figure 3: **Overview of Fluorescence Correlation Spectroscopy (FCS).** **A.** General set-up of a confocal microscope featuring an objective lens with high numerical aperture. A laser is used to focus light on a sample at a particular excitation wavelength. Light emitted from fluorescent species pass through a pinhole before reaching the detector. **B.** Fluorescently-tagged proteins are free to diffuse through the small illuminated volume (confocal volume), resulting in fluctuations in fluorescence intensity as these species pass into the confocal volume and become excited by the laser. **C.** These changes in intensity over time are recorded and used for further analysis such as autocorrelation and photon counting histogram (PCH) (adapted from Kilpatrick & Hill 2016).

Autocorrelation analysis can be conducted on FCS data by use of the following equation for the autocorrelation function, $G(\tau)$, which describes time-dependent decay of fluctuations in fluorescence intensity:

$$G(\tau) = \frac{\langle \delta F(t) \cdot \delta F(t + \tau) \rangle}{\langle F(t) \rangle^2},$$

where F represents the average fluorescence intensity, $\delta F(t)$ represents the change in fluorescence intensity at a particular time (t), and $t + \tau$ represents a later timepoint (Herrick-Davis *et al* 2013). Correlation curves (autocorrelation vs time) are fit either to a 2-D model for lateral diffusion within the plasma membrane, a or 3-D model for diffusion within the cytoplasm (Kilpatrick & Hill 2016). The amplitude of the resulting curve is inversely proportional to the concentration of fluorescent particles while the decay time of $G(\tau)$ is inversely proportional to the rate of diffusion (Figure 4A).

While autocorrelation analysis describes fluorescent fluctuations temporally, PCH describes them by their amplitude (Chen *et al* 1999). The total observation time from FCS recordings is broken down into “bins” which are then plotted against the frequency of photon counts (Herrick-Davis *et al* 2013). (Figure 4B). PCH is used to calculate the average molecular brightness (expressed in counts per second per molecule (cpsm)) of all fluorescent species in the confocal volume. Since molecular brightness is directly proportional to the number of molecules in a cluster, oligomer size can be determined. A dimer would have a molecular brightness twice that of a monomer (Kilpatrick & Hill 2016). A one-component model assumes a homogenous population of a single fluorescent species and allows free measurement of molecular brightness and concentration (Herrick-Davis *et al* 2012). In multicomponent PCH, the molecular brightness is fixed to that of a monomeric, dimeric, or multimeric standard to determine the heterogeneity of the fluorescent species in the sample (Herrick-Davis *et al* 2013).

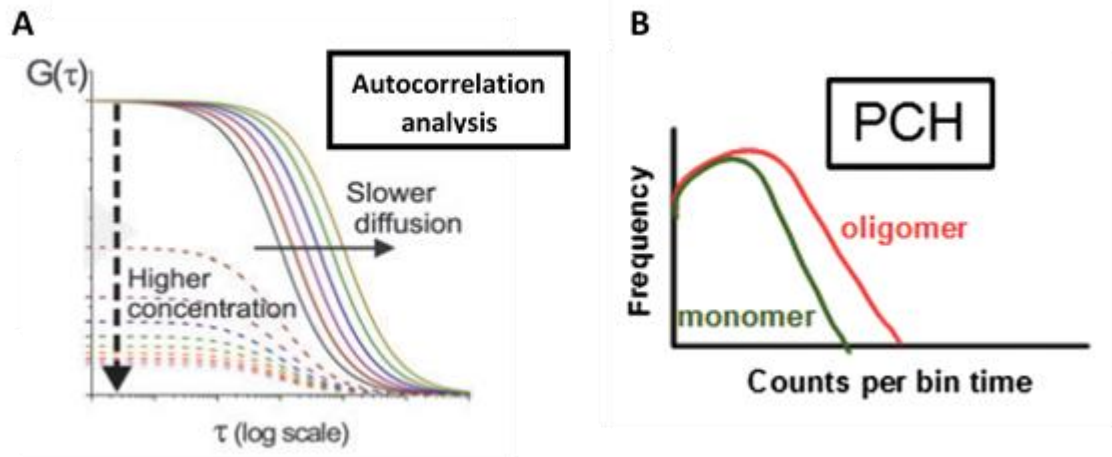


Figure 4: **Autocorrelation analysis and photon counting histogram.** Fluorescence correlation spectroscopy (FCS) recordings can be used for autocorrelation analysis (A) (adapted from Bacia *et al* 2006) and photon counting histogram (PCH) (B) (adapted from Youker & Teng 2014). Autocorrelation curves provide information about the number and diffusion rates of fluorescent particles in the confocal volume, while PCH shows the number of photon counts per “bin” of the total FCS observation period. PCH is used to determine the average oligomer size of fluorescently-tagged particles

1.6 Overview of the Role of Platelets in Hemostasis and Thrombosis

Our lab studies receptors important for platelet activation and aggregation. Platelets are anucleate cells derived from megakaryocytes that are 2-3 μ m and live up to 9 days. Upon vascular injury, platelets come in contact with subendothelial compounds such as collagen and von Willebrand factor. Platelets become activated and change shape, increasing their surface area to facilitate adhesion. They release signaling molecules from dense granules which activates passing platelets and recruits them to the site of injury where they aggregate forming a platelet plug. Molecules released from platelet alpha granules triggers the clotting cascade which leads to the formation of thrombin from prothrombin, the most potent platelet activator (Ghoshal

& Bhattacharyya 2014). Fibrin, by which platelets attach through interaction with activated integrin glycoprotein IIb/IIIa (α IIb β 3), stabilizes the hemostatic plug (Lisman *et al* 2005).

Aside from their normal physiological response to injury in hemostasis, platelets can be activated inappropriately, forming thrombi. Thrombosis is the pathophysiological formation of a clot that can obstruct a vessel and potentially lead to heart attack or stroke (Hou *et al* 2015).

1.7 Platelet Purinergic and Protease-Activated Receptors

The initial contact of platelets with components of the subendothelium following vascular injury involves GPIb/V/IX and GPVI, which interact with von Willebrand factor and collagen, respectively. However, further activation and recruitment of passing platelets to the site of injury to form a stable platelet plug involves signaling through GPCRs (Offermanns 2006). Here, I will focus on two groups of relevance to this study: purinergic and protease-activated receptors.

Human platelets express two purinergic receptors, P2Y1 and P2Y12, which are activated by ADP. P2Y1 is widely found on a variety of cell types including sympathetic and sensory neurons, astrocytes, monocytes, brown adipocytes, gut epithelial cells, and chondrocytes (Abbracchio *et al* 2006). Its expression is low compared to other platelet receptors with only approximately 150 surface binding sites. P2Y1 is important for the initial response to ADP, inducing shape change and weak reversible aggregation through G α q coupling (Hechler & Gachet 2011).

P2Y12 is expressed predominantly, although not exclusively, on platelets with a greater number of binding sites than P2Y1, making it an ideal therapeutic antithrombotic target (Cattaneo 2008). Current clinically effective drugs such as

Clopidogrel target P2Y₁₂ and are routinely administered to patients with acute coronary syndromes and following percutaneous coronary intervention (Sambu & Curzen 2011). The role of P2Y₁₂ in ADP-mediated platelet aggregation is critical physiologically in that its deficiency leads to increased bleeding times in both mice and human patients (Dorsam & Kunapuli 2004). Signaling through P2Y₁₂, coupled to G_{ai}, inhibits adenylyl cyclase, but the resulting decrease in cellular levels of cAMP alone is insufficient for stable aggregation (Hecher & Gachet 2011). Further signaling to activate Akt, through the βγ subunit of the heterotrimeric G protein is required (Kahner *et al* 2006), which is important for activation of integrin αIIbβ₃ that binds fibrinogen (Guidetti *et al* 2015).

Protease-activated receptors (PARs) undergo proteolytic cleavage at their N-termini to reveal a tethered ligand. Both PAR1 and PAR4 are expressed on human platelets, which are stimulated by thrombin, the most potent platelet agonist. PAR1 is sensitive to thrombin and initiates a rapid but temporary response at low concentrations through coupling G_{αq} and G_{α12/13}. It is rapidly internalized and trafficked to the lysosome for degradation. PAR4, which also signals through G_{αq} and G_{α12/13}, is required for a sustained rise in intracellular calcium (Coughlin 2005) and the release of dense granules containing ADP, which activates P2Y₁ and P2Y₁₂ (Holinstat *et al* 2006; Kim *et al* 2002).

While each of these receptors independently contribute to platelet activation and aggregation, they also physically interact having important implications for signaling, as described in the next section.

1.8 Dimerization of Platelet GPCRs

Class A GPCRs expressed on the plasma membrane of platelets, such as Thromboxane A2 receptor, PAR1, PAR4, and P2Y12, have been found to form homo- and heterodimer complexes.

Thromboxane A2 receptor has two isoforms which dimerize along TM1 (Fanelli *et al* 2011). Interestingly, naturally-occurring point mutations in this domain, identified in two separate patients with bleeding disorders, were found to have a reduced tendency to dimerize. Dimerization deficient mutants of both thromboxane A2 receptor (Capra *et al* 2017) and PAR4 (Fuente *et al* 2012) exhibited reduced G α q signaling as measured through IP3 levels and calcium mobilization, respectively. Additionally, PAR4 activation is facilitated by PAR1-assisted cleavage through thrombin-induced heterodimerization (Arachiche *et al* 2013).

Of particular interest and relevance to the work conducted in this thesis, P2Y12 has been reported to homodimerize (Savi *et al* 2006; Zhang *et al* 2014b) but the functional unit remains unclear. Crystal structure of the receptor stabilized by the reversible antagonist AZD1283 revealed a dimer mediated by TM5 (Zhang *et al* 2014b). While the authors did not allude to a dimer in the 2MeSADP agonist-bound structure of P2Y12, the possibility of homodimerization cannot be excluded as the orientation and positioning of TM5 was virtually unchanged relative to the antagonist-bound structure (Zhang *et al* 2014a).

Crystallization of GPCRs is difficult and requires non-physiological conditions to successfully obtain the desired protein which may produce artifacts (Gurevich & Gurevich 2018). For example, P2Y12 was mutated in TM7 at position 294 to increase purification yields (Zhang *et al* 2014b). Additionally, the authors noted that the agonist-bound structure may not reflect the active form of the receptor due to

differences in the positioning of key intracellular domains when compared to β 2AR, which was crystalized with Gas to stabilize its active conformation (Zhang *et al* 2014a).

Another study detected P2Y12 oligomers, dimers, and monomers in both freshly isolated rat platelets and transfected HEK293T cells through immunoblotting (Savi *et al* 2006). This was evidenced by additional bands of higher molecular weights than predicted for the monomeric receptor. Treating cells expressing P2Y12 with the active metabolite of Clopidogrel, an antithrombotic drug and irreversible inhibitor of P2Y12, increased band intensity corresponding to dimers and monomers, and eliminated bands corresponding to oligomers. P2Y12 oligomers, determined to predominantly reside in lipid rafts, were partitioned out of these microdomains by Clopidogrel.

While this mechanism of P2Y12 antagonism was originally interpreted to suggest that the functional unit of P2Y12 is a higher-ordered oligomer (Savi *et al* 2006), it is unclear whether disrupting oligomerization alone is sufficient to eliminate receptor activity. Additionally, because Western blot analysis (as used here) involves cell lysis and disruption of the plasma membrane, solubilized proteins may artificially aggregate (Angers *et al* 2000). Therefore, this technique is limiting in understanding native interactions.

Considering the limitations of previous studies, my lab sought to further understand the oligomer size of P2Y12 in living cells. Using fluorescence correlation spectroscopy (FCS) and photon counting histogram (PCH), we demonstrated for the first time that the predominant species of unstimulated P2Y12 is a monomer on the plasma membrane of HEK293T cells when expressed heterologously (Figure 5;

Barnawi 2017). While we found constitutive agonist-independent P2Y12 homodimers at both the plasma membrane and trans-Golgi network using bimolecular fluorescence complementation (Khan 2015), this may represent only a small subset of receptors.

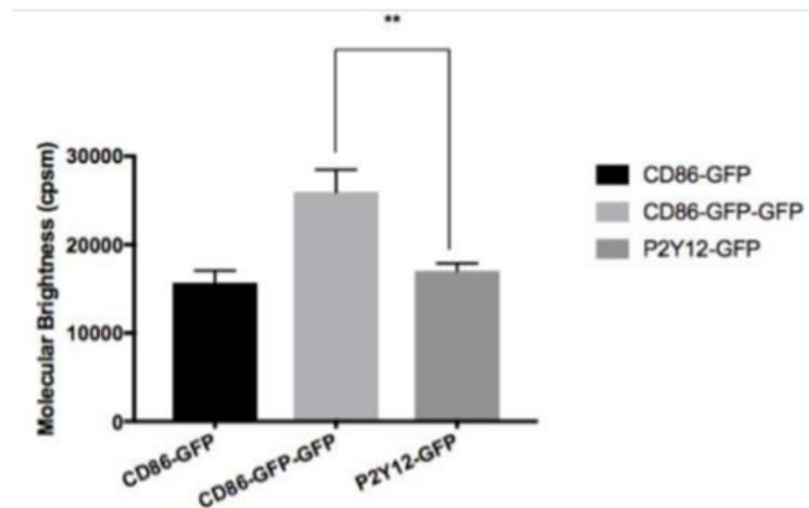


Figure 5: **P2Y12 exists predominately as a monomer on the membrane of live cells.** HEK293T cells were transiently transfected with CD86-GFP (monomeric control), CD86-GFP-GFP (dimeric control), and WT P2Y12-GFP. Molecular brightness was determined at 36 hours post-transfection via FCS and one-component PCH analysis. Error bars represent standard deviation. ** $p < 0.001$, student's t-test. There was no significant difference in molecular brightness between CD86-GFP and WT P2Y12-GFP ($p=0.699$, student's t-test) (adapted from Barnawi 2017).

In addition to homodimerization, P2Y12 has also been found to form heterodimeric structures which are important for intracellular signaling events. My lab has found that P2Y12 physically associates with PAR4 in a saturation BRET assay. These interactions are increased in the presence of PAR4-specific agonist AYPGKF, decreased in the presence of P2Y12 antagonist MeSAMP, and demonstrate functional

relevance as disrupting P2Y12-PAR4 heterodimers decreases the levels of phosphorylated Akt in HEK293T cells (Khan *et al* 2014).

1.9 Naturally-Occurring Mutant Variants of P2Y12

Two naturally occurring mutant variants of P2Y12 have been identified in a patient with congenital bleeding disorder: R256Q and R265W. A point mutation resulted in an arginine (R) to glutamine (Q) substitution at amino acid (a.a.) 256 or an arginine (R) to tryptophan (W) substitution at a.a. 265, respectively. The patient was found to be a compound heterozygote which means each mutation is located in the coding region for P2Y12 on a separate chromosome. Interestingly, the mutant receptors on platelets isolated from the patient were found to have normal surface expression and agonist binding but defective G α i coupling (Cattaneo *et al* 2003). It is interesting to note the location of the mutations: one is located in the sixth transmembrane region (TM6) while the other is located on the third extracellular loop (ECL3) (Figure 6). This is not expected to affect G α i coupling because the heterotrimeric G protein interacts with the receptor on the cytosolic surface. It is possible that altered dimerization of the receptor is affecting its ability to signal.

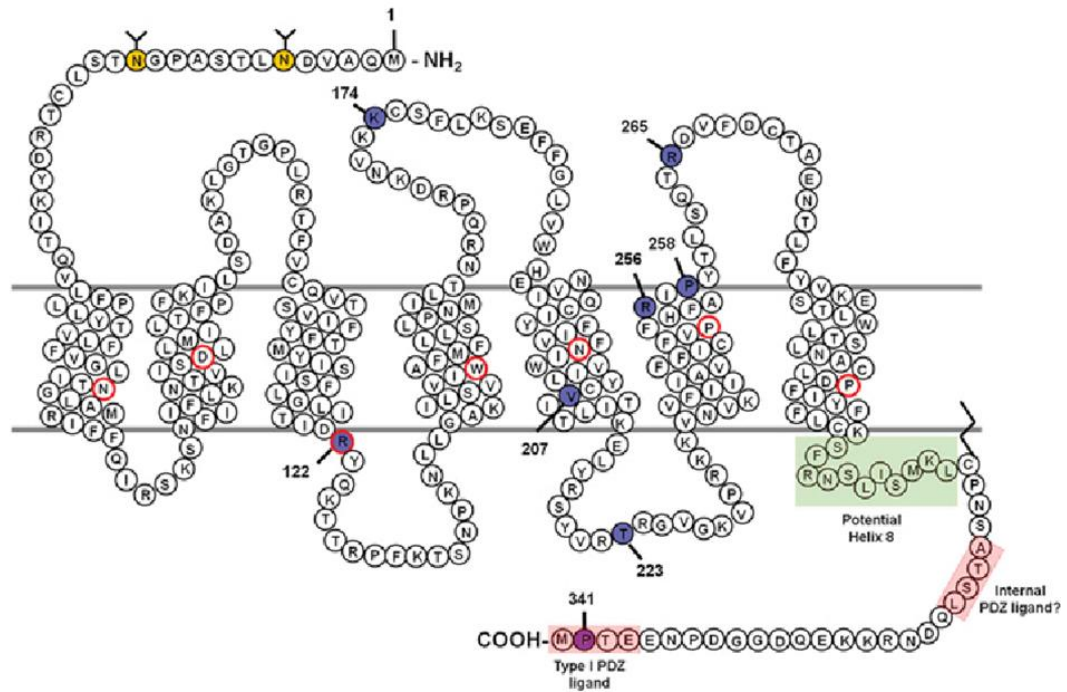


Figure 6: **Snake plot of the human purinergic platelet receptor, P2Y12.** P2Y12 is a class A G-protein-coupled receptor (GPCR) expressed mainly on platelets and is important for their aggregation. Human P2Y12 is made up of 342 amino acids with the N-terminus oriented extracellularly and the C-terminus, cytosolically. Here, conserved transmembrane (TM) residues are circled in red, while two N-linked glycosylation sites found to be important for signal transduction are shown in yellow. Amino acids in blue represent documented positions that have been mutated in patients with a bleeding phenotype (adapted from Cunningham *et al* 2013).

Recently, my lab studied these mutant variants in isolation (Figure 7) to determine if each independently contributes to the observed functional G_{ai}-coupling defect in platelets, and if they exhibited any structural differences from the wild-type receptor. Using fluorescence correlation spectroscopy, we found that P2Y12 mutant variants, R256Q and R265W had an increased tendency to homodimerize relative to WT P2Y12 (Figure 8). Furthermore, we found that P2Y12R256Q expressed in

isolation on HEK293T cells failed to decrease forskolin-induced cAMP activity, indicating an inability to properly couple G α i (Figure 9). It is possible that the observed increase in self-association alters either the interface responsible for direct physical contact with the heterotrimeric G protein, or the receptor's guanine nucleotide exchange factor (GEF) activity. Interestingly, the increased homodimerization defect appears to be more severe in P2Y12R265W than P2Y12R256Q. Therefore, I decided to further investigate structural and functional properties of the P2Y12 mutant R265W in this thesis.

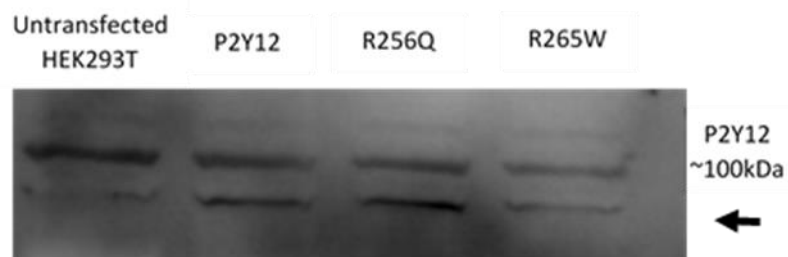


Figure 7: P2Y12 expression in HEK293T cells stably expressing WT P2Y12 or P2Y12 mutant variants R256Q or R265W. HEK293T cells stably expressing Flag-tagged WT P2Y12, or one of two P2Y12 mutant variants, R256Q or R265W, were grown to 70% confluency, serum starved for 12 hours, and lysed. Untransfected HEK293T cells were lysed and used as a negative control. Lysates were run on 10% SDS-polyacrylamide gel and immunoblotted for P2Y12 (1:100, Santa Cruz Biotechnologies).

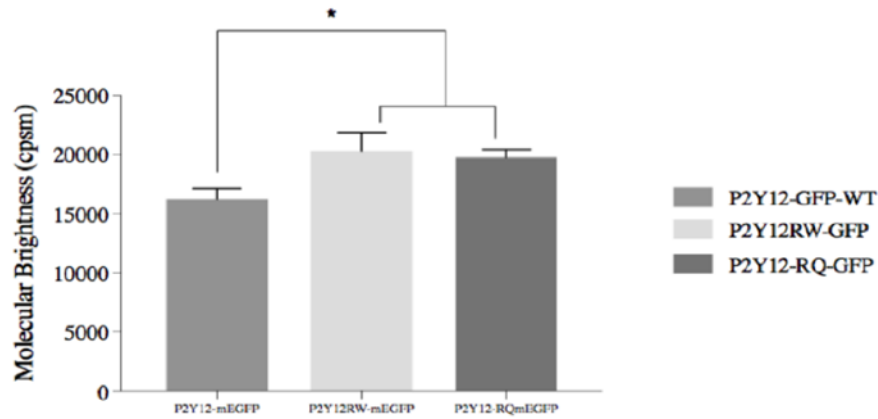


Figure 8: **P2Y12 mutant variants R265W and R256Q form a higher proportion of homodimers than WT P2Y12.** HEK293T cells were transiently transfected with GFP-tagged WT P2Y12, or mutant variants R265W or R256Q. Molecular brightness was determined at 36 hours post-transfection via FCS and one-component PCH analysis. Error bars represent standard deviation. * $p < 0.01$, student's t-test (adapted from Barnawi 2017).

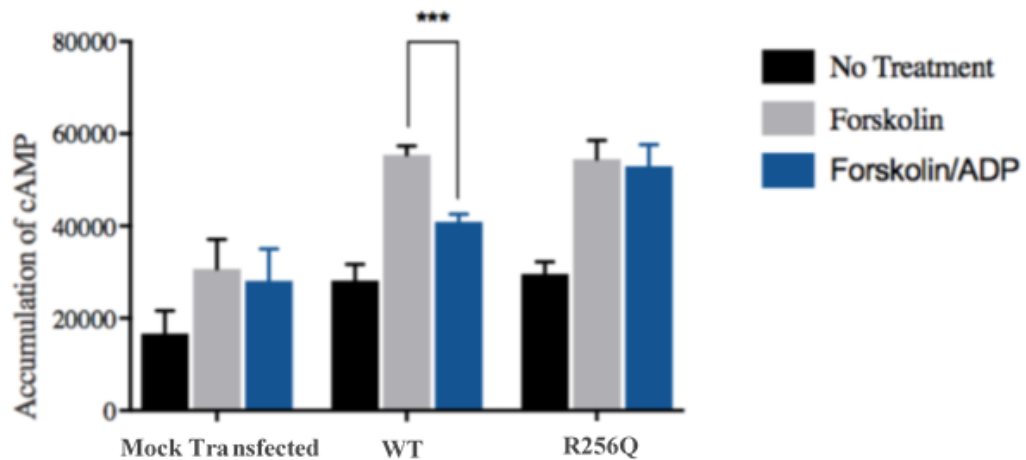


Figure 9: **P2Y12 mutant variant R256Q failed to activate G α i.** HEK293T cells were transiently co-transfected with pGloSensor-20F cAMP plasmid and pcDNA (mock), WT P2Y12, or P2Y12R256Q. Cells were either left untreated, or treated with forskolin alone (10 μ M) or in the presence of ADP (10 μ M), and the accumulation of cAMP was measured by luminescence (RLU). Presented is the mean \pm SD of three independent experiments, *** $p < 0.0001$, ANOVA (adapted from Barnawi 2017).

Another mutant variant of P2Y₁₂ has been recently discovered by our collaborators (Satya Kunapuli and John Kostyak; see Kostyak *et al* 2018) at Temple University, Philadelphia, PA in an individual with no history of bleeding. A point mutation resulted in an amino acid substitution from aspartic acid (D) to asparagine (N) at position 121 in the asparagine-arginine-tyrosine (DRY) motif (Kostyak *et al* 2018). While GPCRs are diverse and share little sequence homology, this motif is highly conserved. This region has been shown to participate in receptor conformational states, trafficking, and interaction with G protein. The central arginine of the motif has been found to form an “ionic lock” with a glutamic acid residue (Glu) in TM6 of rhodopsin and a salt bridge with the adjacent aspartic acid (Glu in rhodopsin) of multiple receptors including β 2AR and adenosine A_{2A}. These ionic interactions are proposed to maintain the receptor in an inactive conformation (Nygaard *et al* 2009).

Platelets isolated from the individual with D121N mutation in P2Y₁₂ are virtually nonresponsive to ADP and lack the ability to aggregate. This is interesting in that the patient is heterozygous for the mutation, which means they should express a functional wild-type receptor to compensate (Kostyak *et al* 2018). The apparent dominant negative phenotype of this mutant variant may be explained through dimerization with the wild type receptor, precluding its function.

A patient homozygous for an arginine (R) to cysteine (C) mutation at the adjacent residue, 122, of P2Y₁₂ was similarly deficient in ADP-dependent platelet aggregation. While ADP-mediated signaling was impaired, the mutant maintained a level of basal activity similar to the WT receptor as measured through inhibition of cAMP. Interestingly, in the absence of agonist, this particular P2Y₁₂ mutant was

internalized more rapidly and found to colocalize with lysosomal markers, suggesting subsequent degradation as opposed to normal recycling to the plasma membrane (Patel *et al* 2014).

Here, I aimed to characterize the functional consequences of an R to W substitution at 265, and independently a D to N substitution at 121 of P2Y₁₂. I also investigated whether these P2Y₁₂ mutants self-associate in an altered manner compared to the WT receptor, and whether they maintain the ability to heterodimerize with PAR4.

Chapter 2

MATERIALS AND METHODS

2.1 Cell Culture

HEK293T cells were grown in 1x DMEM without L-glutamine (Corning), and supplemented with 10% fetal bovine serum (FBS) (Gemini), and 1% penicillin-streptomycin (HyClone).

2.2 Akt Activation Experiments

2.2.1 Plasmid Constructs

Flag-P2Y12 and HA-PAR4 plasmid constructs were created by subcloning human P2Y12 into Flag pcDNA 3.0 and human PAR4 into HA pcDNA 3.0, respectively (gift from Dr. Ji-Fang Zhang, Thomas Jefferson university, Philadelphia, PA).

Mutant P2Y12 Flag-R265W and Flag-D121N were created using QuikChange II site-directed mutagenesis kit (Agilent) using the Flag-P2Y12 plasmid construct as a template. Success of mutagenesis was confirmed by DNA sequencing (Genewiz).

Mutagenic primers were designed using the QuikChange Primer Design Program at: www.agilent.com/genomics/qcpd. The designed oligos (obtained from Integrated DNA Technologies) were as follows:

P2Y12R265W (C to T mutation at nucleotide 793):

5'- CAC CCT GAG CCA AAC CTG GGA TGT CTT TGA CTG -3' (forward)

5'- CAG TCA AAG ACA TCC CAG GTT TGG CTC AGG GTG -3 (reverse)
P2Y12D121N (G to A mutation at nucleotide 361):

5'- CCT GGG ACT GAT AAC TAT CAA TCG CTA CCA GAA GAC C -3'
(forward)

5'- GGT CTT CTG GTA GCG ATT GAT AGT TAT CAG TCC CAG G -3'
(reverse)

2.2.2 Generation of Stable Cell Lines

HEK293T cells were co-transfected with each of 14µg HA-PAR4 and Flag-P2Y12, Flag-P2Y12R265W, or Flag-P2Y12D121N constructs using TransIT293 transfection reagent (Mirus). Cells were selected for 3 weeks using 400µg/mL Hygromycin B (Roche) for Flag-tagged P2Y12, P2Y12R265W, and P2Y12D121N, and 1000µg/mL Geneticin (Invitrogen) for HA-tagged PAR4. Expression was confirmed via Western blot analysis with antibodies against P2Y12 (1:100, Santa Cruz Biotechnologies) and PAR4 (1:750, Cell Signaling Technologies). The stable cells were then maintained in 200µg/mL Hygromycin and 500µg/mL Geneticin.

2.2.3 Preparation of Cells and Western Blotting

HEK293T cells stably expressing Flag-P2Y12 and HA-PAR4, Flag-P2Y12R265W and HA-PAR4, and Flag-P2Y12D121N and HA-PAR4 were grown to 70-80% confluency and then serum starved for 12-13 hours. Cells were left untreated, or treated with ADP (10µM, Chronolog Corp) or AYPGKF (400µM, Biopeptek) for 10 minutes at 37°C and then lysed with 1X lysis buffer (150 mM NaCl, 10 mM Tris, 0.5% deoxycholic acid, 5 mM EDTA, 0.5 mM PMSF, pH 7.4) with 1% Triton X (Sigma) and 1x protease inhibitor (Roche). 60µg of lysates were resolved onto 10%

SDS-polyacrylamide gel, transferred to 0.2µm PVDF membrane and immunoblotted using antibodies against phospho-Akt(S473) (1:500, Cell Signaling Technologies) or total-Akt (1:1500, Cell Signaling Technologies). Immunoblots were developed using chemiluminescence and captured in the ChemiDoc Imaging System (Bio-Rad).

Relative densities of p-Akt and total Akt were determined using ImageJ software. The ratio of the relative densities of p-Akt to total Akt were calculated for each experiment.

2.2.4 Statistical Analysis

Data was imported into Microsoft Excel for each experiment, and used to generate bar graphs displaying the mean +/- SEM. Unpaired student's t-tests were conducted comparing the mean ratio of p-Akt to total Akt between untreated HEK293T cells stably co-expressing PAR4 and WT P2Y12, and cells stably co-expressing PAR4 and either one of two P2Y12 mutant variants R265W or D121N.

2.3 Fluorescence Correlation Spectroscopy (FCS) and Photon Counting Histogram (PCH) Experiments

2.3.1 Plasmid Constructs

The CD86-GFP and CD86-GFPGFP constructs (gift from Prof. Graeme Milligan, University of Glasgow) contain the coding sequence for the monomeric plasma membrane receptor, CD86, fused to either one eGFP (monomeric control) or two eGFP in tandem (dimeric control), respectively. The eGFP used in these constructs contains an A206K mutation to prevent dimerization of the fluorescent protein tag (Zacharias *et al* 2002).

P2Y12-GFP was created by subcloning human P2Y12 into pEGFP-N2 vector. P2Y12R265W-GFP and P2Y12D121N-GFP were created using QuickChange II site-directed mutagenesis kit (Agilent) using P2Y12-GFP as a template. Success of mutagenesis was confirmed by DNA sequencing (Genewiz). The oligos used to create the P2Y12 mutant variants are detailed in section 2.2.1

2.3.2 Cell Culture and Transfection

2.3.2.1 Homomeric Interactions of Wild-Type P2Y12 and Mutant Variants, R265W and D121N

HEK293T cells were seeded in laminin-coated (25ng/ μ L in PBS) 4-well Nunc Lab-Tek II 1.5mm Chambered Coverglass (Thermo Scientific) at a density of 15,000 cells in 0.5 mL of DMEM media supplemented with 10% FBS and allowed to grow for 7-8 hours prior to transfection. Cells were transfected with 20ng of CD86-GFP monomeric control, CD86-GFPGFP dimeric control, P2Y12-GFP, P2Y12R265W-GFP or P2Y12D121N-GFP in OptiMEM reduced serum media (Gibco) with TransIT293 transfection reagent (Mirus) in 1:3 ratio of plasmid to transfection reagent. Cells were assayed at approximately 36 hours post transfection. DMEM media was replaced with Live Cell Imaging Solution (Life Technologies), warmed to 37°C immediately prior to confocal imaging, and FCS and PCH analysis.

2.3.2.2 Heteromeric Interactions of P2Y12 Mutant Variant R265W with PAR4

HEK293T cells were seeded in laminin-coated 4-well Nunc Lab-Tek II 1.5mm Chambered Coverglass at a density of 15,000 cells per 0.5 mL of DMEM media supplemented with 10% FBS and allowed to grow for 24 hours prior to transfection. Cells were transfected with 20ng CD86-GFP (monomeric control), CD86-GFPGFP

(dimeric control), P2Y12-GFP, or P2Y12R265W-GFP, or co-transfected with 20ng P2Y12R265W-GFP and increasing amounts of HA-PAR4 (20ng to 360ng) in a P2Y12R265W to PAR4 ratio of 1:1, 1:4, and 1:16. pcDNA was added to balance the total DNA transfected into each well. Cells were assayed at approximately 36 hours post transfection. DMEM media was replaced with Live Cell Imaging Solution (Life Technologies), warmed to 37°C immediately prior to live cell confocal imaging, and FCS and PCH analysis.

2.3.3 System Settings for FCS and PCH Analysis

Live cell confocal imaging and fluorescence correlation spectroscopy (FCS) were conducted using a LSM880 confocal microscope (Zeiss) equipped with a FAST Airyscan detector at the Delaware Biotechnology Institute in Newark, DE. Cells were observed using a C-Apochromat 40x water-immersion objective lens with the collar adjusted at 1.7, and illuminated using an argon laser for single-photon excitation. 488nm, laser power of 0.2%, was used for excitation of eGFP-tagged receptors. Emitted fluorescence passed through a pinhole of 32 μ m before reaching the detector. Measurements were taken near the center of the cell on the plasma membrane, which was determined as the focal plane at which the count rate was maximal. Cells were selected with an average plasma membrane count rate between 50 and 200 kHz, and regions of the cells exhibiting filipodia were avoided. FCS recordings of each cell were taken for 5 consecutive repetitions of 10 seconds each, for a total measurement time of 50s. An autocorrelation bin time of 0.2 μ s was used. Cells were kept in a humidifying chamber at 37°C and 5% CO₂ throughout the FCS measurements.

To determine average molecular brightness within the illuminated confocal volume, one component photon counting histogram (PCH) analysis was performed.

Each 10s interval of each 50s observation period per cell from the FCS recordings was broken down into bins of 20 μ s. Histograms were constructed with the photon counts on the x axis and the frequency on the y axis. The molecular brightness and concentration were left free, while the first order correction was fixed at a value determined during pinhole alignment prior to the start of each experiment. The background was set to 455.

2.3.4 Pinhole Alignment

The system was turned on and allowed to warm up for at least 30 minutes prior to imaging and data collection. Rhodamine 123 (Invitrogen) was diluted to 1.6nM in water in 4-well Nunc Lab-Tek II 1.5mm Chambered Coverglass. The focal plane was set to 30 microns from the coverglass in the center of the well. The pinhole was aligned in the x and y plane using the adjustment tool in Zen2.1 Black software (Zeiss). FCS measurements were taken using 488nm excitation and 2% laser power within a 100s observation period of 10 consecutive 10-second repetitions. The first order correction was allowed to be free; the values for the 10 repetitions were averaged and then used to fix the first order correction for PCH analysis of the cells.

2.3.5 Statistical Analysis

Data analysis was conducted using ZEN 2.1 Black software (Zeiss). Molecular brightness data was then imported into Microsoft Excel and either graphed as the mean +/- SEM of technical replicates, or normalized to the molecular brightness of monomeric control, CD86-GFP for each experiment and then graphed as the mean fold change in molecular brightness +/- SEM of independent experiments. Paired

student's t-tests were conducted comparing the mean fold change in molecular brightness between WT P2Y12 and each P2Y12 mutant variant, R265W and D121N.

2.4 Gai-Coupling of P2Y12 Receptor

2.4.1 Plasmid Constructs

pGloSensor-20F cAMP plasmid (GenBank accession number: EU770615) was obtained from Promega (Madison, WI). This construct contains the coding region for a mutant form of the firefly, *Photinus pyralis*, luciferase fused to a cAMP-binding domain. The binding of cAMP causes a conformational change, resulting in an increased output of light which correlates to the levels of cAMP present in live cells (Figure 10).

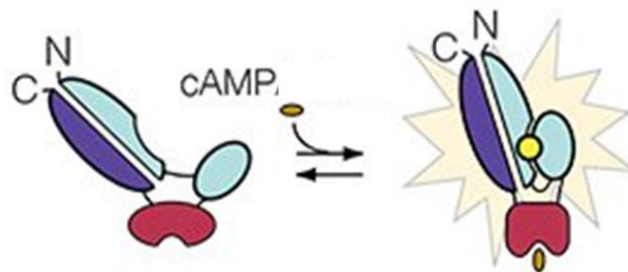


Figure 10: **Schematic of GloSensor Technology.** pGloSensor-20F cAMP plasmid (Promega) allows for heterologous expression of a modified form of the firefly (*Photinus pyralis*) luciferase containing a binding site for cAMP. Analyte binding leads to a conformational change that promotes an increase in luminescence activity. Therefore, the magnitude of this increased light output is directly proportional to the amount of cAMP present in live cells (adapted from Fan *et al.* 2008).

P2Y12-GFP was created by subcloning human P2Y12 into pEGFP-N2 vector. P2Y12R265W-GFP and P2Y12D121N-GFP were created using QuickChange II site-directed mutagenesis kit (Agilent) using P2Y12-GFP as a template. Success of mutagenesis was confirmed by DNA sequencing (Genewiz). The oligos used to create the P2Y12 mutant variants are detailed in section 2.2.1.

2.4.2 GloSensor cAMP Assay

HEK 293T cells were seeded into 6 well plates and co-transfected with 2 μ g or 5 μ g each of pGloSensor-20F cAMP plasmid and either empty pcDNA3.0 vector (mock transfection), P2Y12-GFP, P2Y12R265W-GFP, or P2Y12D121N-GFP. Cells were lifted 36 to 72 hours post-transfection, and equilibrated in 88% CO₂-independent media (Gibco), 10% FBS (Gemini), and 2% GloSensor cAMP reagent stock solution (GloSensor cAMP reagent (Promega) dissolved in 10mM HEPES buffer, pH 7.5, as per manufacturer's instructions) at room temperature for 2 hours with mixing every 15 min. Cells were then transferred into a clear, flat-bottom 96 well plate at 15,000 cells/100 μ L per well. The cells were left untreated, or treated either with 0.4 μ M forskolin alone or with 0.4 μ M ADP (Chronolog Corp) for 30 minutes at room temperature. The relative levels of cAMP in the cells were determined by measuring luminescence using the GloMax Multi-detection plate reader (Promega). Data was normalized to percent forskolin-induced cAMP activity as follows: cAMP levels of untreated cells were subtracted from that of forskolin-treated cells and cells treated with both forskolin and ADP. Then the cAMP levels of forskolin treated cells were taken as 100% and cAMP levels in cells treated with both forskolin and ADP were taken as a percent of the forskolin-treated cells.

2.4.3 Statistical Analysis

Raw data was imported into Microsoft Excel, and bar graphs were generated displaying the mean percent forskolin-induced cAMP activity \pm SEM. Unpaired student's t-tests were conducted comparing the mean percent forskolin-induced cAMP activity between ADP-treated cells expressing WT P2Y₁₂, and each of the two P2Y₁₂ mutant variants, R265W and D121N.

Chapter 3

RESULTS

3.1 Activation of Akt by P2Y12 Mutant Variants

3.1.1 Background

Activation of Akt is an important step in platelet aggregation and adhesion (Li *et al* 2010). It is activated downstream of PI3K through independent phosphorylation at two sites: serine473 and threonine308. Of the three known isoforms, Akt1 and Akt2 are expressed in platelets, although not exclusively (Woulfe 2010). Evidence supports that deficiencies in Akt1 (Chen *et al* 2004) and Akt2 (Woulfe *et al* 2004) impair granule secretion and fibrinogen binding following platelet stimulation by thrombin or PAR4-agonist, respectively. Having higher expression in mouse platelets, Akt2 deficiency was found to impede the formation of stable thrombi after carotid artery injury *in vivo* (Woulfe *et al* 2004).

Both ADP and thrombin contribute to Akt activation in platelets (Woulfe 2010), although ADP-mediated activation is weaker (Kim *et al* 2006). Thrombin stimulation promotes the Gq-mediated release of dense granules containing ADP that in-turn activates P2Y12 and contributes to Akt activation. This is supported in that PAR-stimulated platelets treated with Gq-inhibitor had diminished levels of phosphorylated Akt, which were restored to normal levels through supplemented Gi signaling (Kim *et al* 2006). Although Gi signaling is important for thrombin-mediated Akt activation, PAR4 can independently activate Akt when treated with high

concentrations of thrombin or AYPGKF (PAR4 agonist) as demonstrated in platelets from P2Y12 knock-out mice (Xiang *et al* 2010). P2Y12 signaling activates Akt through Gi pathways independent of arrestin recruitment, as P2Y12 inhibition in platelets from arrestin-2 knock-out mice further decreased phosphorylated Akt levels. PAR4-mediated activation of Akt, on the other hand, is partly dependent on arrestin-2 (Li *et al* 2011). While P2Y12 and PAR4 can each independently activate Akt, synergy between the two receptors, and arrestin-mediated signaling, appear to be required for maximal Akt activation.

More recently, my lab has found that the physical association between P2Y12 and PAR4 contributes to arrestin-mediated Akt activation in response to PAR4 agonist. Arrestin-2 was found to co-immunoprecipitate with PAR4 only when co-expressed with P2Y12 in HEK293T cells, suggesting a mechanism by which P2Y12 recruits arrestin-2 to PAR4 (Khan *et al* 2014). Another study demonstrated that PAR4 drives the internalization of P2Y12 by heterodimerization which is required for activating Akt (Smith *et al* 2017).

R265W and D121N are two naturally occurring mutant variants of P2Y12. The first was identified in a patient with a mild bleeding disorder who was compound heterozygous for this mutant variant and another, R256Q (Cattaneo *et al* 2003). The second was identified in a heterozygous individual with no history of bleeding (Kostyak *et al* 2018). Platelets from both individuals have a severe aggregation defect in response to ADP (Cattaneo *et al* 2003; Kostyak *et al* 2018).

How these P2Y12 mutant variants may influence Akt activation has not been investigated. It is possible that the phenotype exhibited in these individuals is the

result of aberrant Akt activation, which could also be dependent on the ability of these receptors to heterodimerize with PAR4 (explored in section 3.2).

3.1.2 P2Y12 Mutant Variants R265W and D121N Have Increased Constitutive Activity in Phosphorylation of Akt

I first created HEK293T cell lines, stably co-expressing HA-tagged PAR4 and either Flag-tagged WT P2Y12, or Flag-tagged P2Y12 mutant variants R265W or D121N (Figure 11).

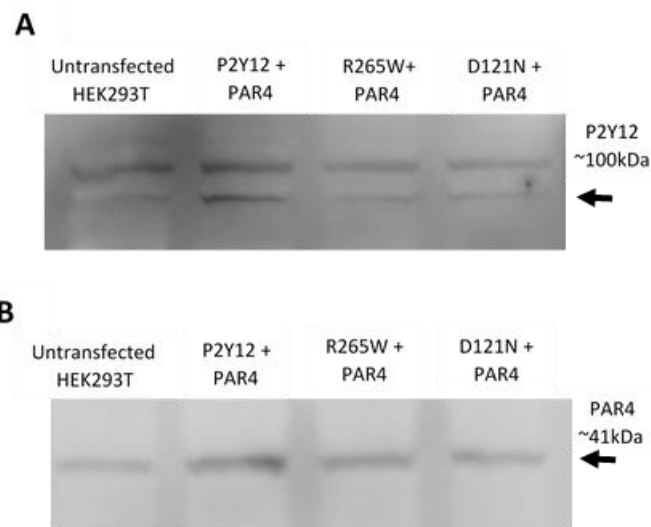


Figure 11: **Confirmation of P2Y12 and PAR4 expression in HEK293T stable cell lines.** HEK293T cells were co-transfected with HA-PAR4, and either WT Flag-P2Y12, Flag-P2Y12R265W, or Flag-P2Y12D121N. Cells were selected in hygromycin (400 μ g/mL) and geneticin (1000 μ g/mL) for 3 weeks, and then maintained in lower concentrations of hygromycin (200 μ g/mL) and geneticin (500 μ g/mL). Stables were grown to 70% confluency in 6-well plates, serum-starved for 12 hours, lysed, and run on a 10% SDS-polyacrylamide gel. An untransfected HEK293T cell lysate was run as a negative control. Immunoblots were probed for (A) P2Y12 (1:100, Santa Cruz Biotechnology) or (B) PAR4 (1:750, Cell Signaling Technologies), and developed using a ChemiDoc imaging system (Bio-Rad).

In order to determine if P2Y12 mutant variants R265W and D121N alter the activation of Akt, I quantified the levels of p-Akt relative to total Akt in these stable cell lines via Western blot and ImageJ density analysis. As expected, we found an increase in p-Akt levels in HEK293T cells stably co-expressing PAR4 and wild type P2Y12 in response to P2Y12 agonist, ADP (10 μ M) (Figure 12 A & B), and PAR4-specific agonist, AYPGKF (400 μ M) (additional preliminary data not shown). Interestingly, in the absence of agonist, HEK293T cells stably expressing PAR4 with either P2Y12 mutant variant R265W or D121N, exhibited higher levels of phosphorylated Akt than cells stably expressing PAR4 and WT P2Y12 ($p < 0.01$, Figure 12A). The increased levels of p-Akt exhibited in untreated cells expressing P2Y12 mutant variants R265W or D121N are not due to higher heterologous expression of these receptors relative to those expressing WT P2Y12 (Figure 11A).

ADP (10 μ M) significantly increased p-Akt levels in HEK cells stably co-expressing PAR4 and P2Y12D121N ($p = 0.04$), but not P2Y12R265W. (Figure 12A). In a single experiment, I found that treating HEK cells co-expressing PAR4 and either P2Y12R265W or P2Y12D121N with PAR4 specific agonist, AYPGKF (400 μ M) did not increase p-Akt levels (additional preliminary data not shown).

Previously, we have found that the physical association between P2Y12 and PAR4, which is increased in the presence of PAR4-agonist AYPGKF, is important for maximal Akt activation (Khan *et al* 2014). Constitutive activity in the P2Y12 mutant variants, R265W and D121N, may be explained by agonist-independent interaction with PAR4. Therefore, I next sought to test the possibility that these P2Y12 mutant variants heterodimerize with PAR4 in unstimulated cells.

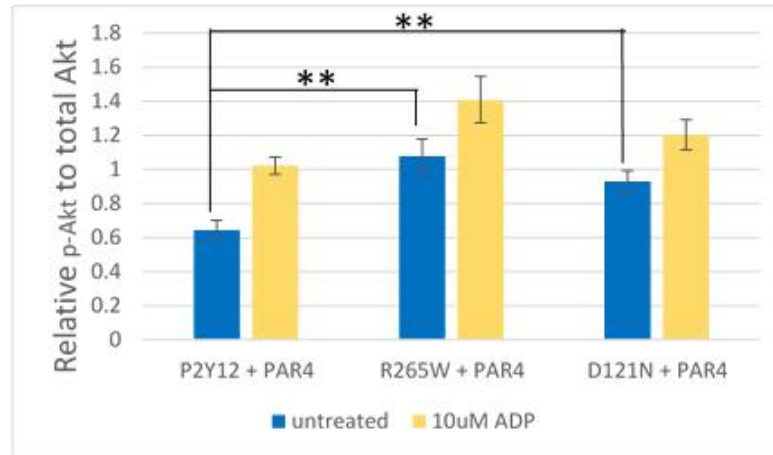
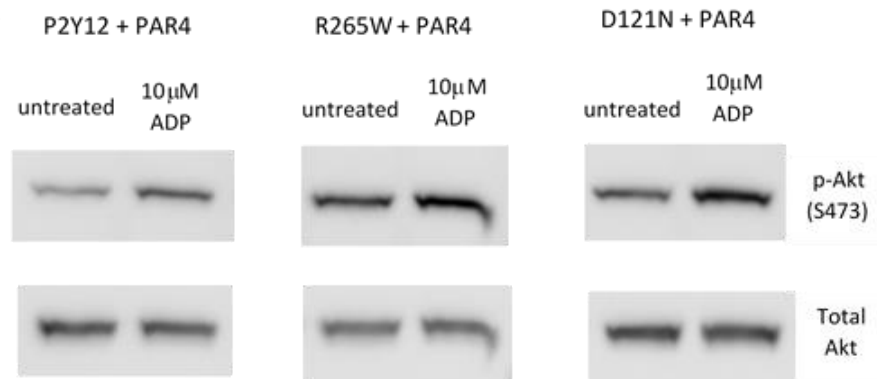
A**B**

Figure 12: Mutant variants of P2Y12, R265W and D121N, have increased constitutive Akt phosphorylation. Stable HEK293T cell lines, co-expressing PAR4 and WT P2Y12 or one of two P2Y12 mutant variants, R265W or D121N, were grown to 70% confluency and serum starved for 12 hours. Cells were left untreated or treated with ADP (10 μ M) for 10 minutes at 37°C. Presented is the quantification of p-Akt normalized to total Akt +/- SEM from 5 independent experiments, ** p<0.01 unpaired t-test (**A**). A representative blot using antibodies against phospho-Akt(S473) (1:500, Cell Signaling Technologies) and total Akt (1:1500, Cell Signaling Technologies), is shown (**B**).

3.2 Structural Analysis of P2Y12 Mutant Variants: Investigating Homo- and Heterodimerization

3.2.1 Background

I found increased Akt activation in untreated HEK293T cells co-expressing one of two P2Y12 mutant variants R265W or D121N, with PAR4. One possible mechanism is through agonist-independent heterodimerization of these receptors. Our lab has previously demonstrated that arrestin-mediated Akt phosphorylation is dependent on the physical association of wild-type P2Y12 and PAR4 (Khan *et al* 2014).

Before exploring potential heterodimerization with PAR4, I wanted to assess the potential of P2Y12 mutant variants R265W and D121N to self-associate in isolation. P2Y12 has been proposed to exist as a functional oligomer (Savi *et al* 2006), and has been crystalized as a homodimer (Zhang *et al* 2014b). While my lab has demonstrated the existence of constitutive P2Y12 homodimers (Khan 2015), we found that the predominant species is a monomer on the plasma membrane of live cells. Interestingly, we found that two mutant variants of P2Y12 (R256Q and R265W), identified in a patient with a mild bleeding disorder, exhibited increased homodimerization compared to the wild-type receptor (Barnawi 2017). Platelets from another individual, heterozygous for a novel P2Y12 mutant D121N, were found to have a severe aggregation defect (Kostyak *et al* 2018). This phenotype may be explained by a change in the dimerization potential of P2Y12D121N, which in-turn inhibits normal functioning of wild-type P2Y12.

Here, I first confirmed the increased homodimerization of P2Y12R265W and then investigated the dimerization potential of P2Y12D121N. Second, I investigated P2Y12R265W ability to associate with PAR4 using a competition assay.

3.2.2 P2Y12 Mutant Variant R265W, but Not D121N, Forms Increased Homodimers

In order to investigate the oligomeric state of two P2Y12 mutant variants, R265W and D121N, I used fluorescence correlation spectroscopy (FCS) and one-component photon counting histogram (PCH) in live cells (see chapter 1 section 5 for more detail on these techniques).

HEK293T cells were transiently transfected with wild type P2Y12, P2Y12R265W and P2Y12D121N tagged with a non-self-associating eGFP (Zacharias *et al* 2002). Cells transfected with monomeric receptor CD86 tagged with either one eGFP (monomeric control) or two eGFP in tandem (dimeric control) served as a point of reference. Before conducting FCS and PCH analysis at 36-hours post-transfection, I imaged the cells by confocal microscopy (Zeiss LSM880) to confirm cell viability and receptor surface expression (Figure 13). Since FCS is most accurately conducted at low concentrations of fluorescently tagged species (Vischer *et al* 2015), I selected cells exhibiting low eGFP expression as defined by a count rate between 50 and 200kHz.

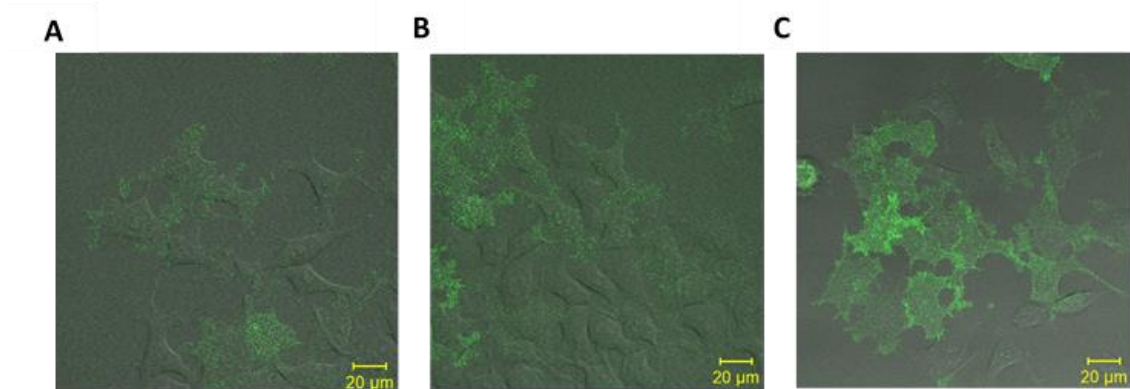


Figure 13: Live cell imaging of HEK293T cells expressing P2Y12 eGFP constructs. HEK293T cells were transiently transfected with eGFP-tagged WT P2Y12 (A), or P2Y12 mutant variants R265W (B) or D121N (C) and imaged by confocal microscopy (Zeiss LSM880) at 36-hours using a 40x water-immersion lens. Zen Black 2.1 software (Zeiss) was used to process the fluorescent and DIC merged images as shown. Yellow scale bar, 20 μ m.

I was able to replicate previous experiments from my lab showing that P2Y12 mutant variant R265W forms increased homodimers relative to the wild type receptor (approaching significance at $p=0.07$; paired t-test). The average molecular brightness of P2Y12R265W was approximately 1.2-fold higher than that of wild type P2Y12 (Figure 14).

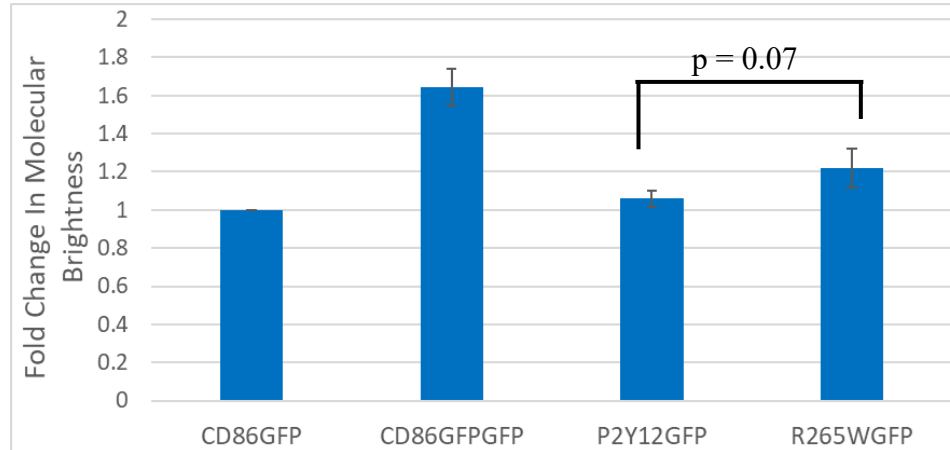


Figure 14: **P2Y12 mutant variant R265W has tendency towards increased homodimerization.** HEK293T cells were transiently transfected with CD86-GFP (as a monomeric control), CD86-GFPGFP (as a dimeric control), P2Y12-GFP or P2Y12R265W-GFP and analyzed by FCS and PCH at 36 hours post-transfection. Molecular brightness was measured to determine the oligomeric state of the receptors, which was normalized to the monomeric control (CD86-GFP, set to 1). Presented is the mean of four independent experiments +/- SEM; $p = 0.07$, paired student's t-test.

As a possible explanation for the apparent dominant negative phenotype exhibited in a patient heterozygous for an aspartic acid to asparagine substitution at amino acid 121 in P2Y12 (Kostyak *et al* 2018), we proposed that P2Y12D121N may form increased homodimers. Surprisingly we did not find a homodimerization defect in this variant as the fold difference in average molecular brightness of HEK293T cells transiently transfected with GFP-tagged P2Y12D121N was not significantly different from that of cells expressing GFP-tagged wild type receptor ($p > 0.05$, paired t-test). (Figure 15). While this mutant variant is unable to self-dimerize, it may be able to associate with wild type P2Y12. Future studies will investigate this possibility.

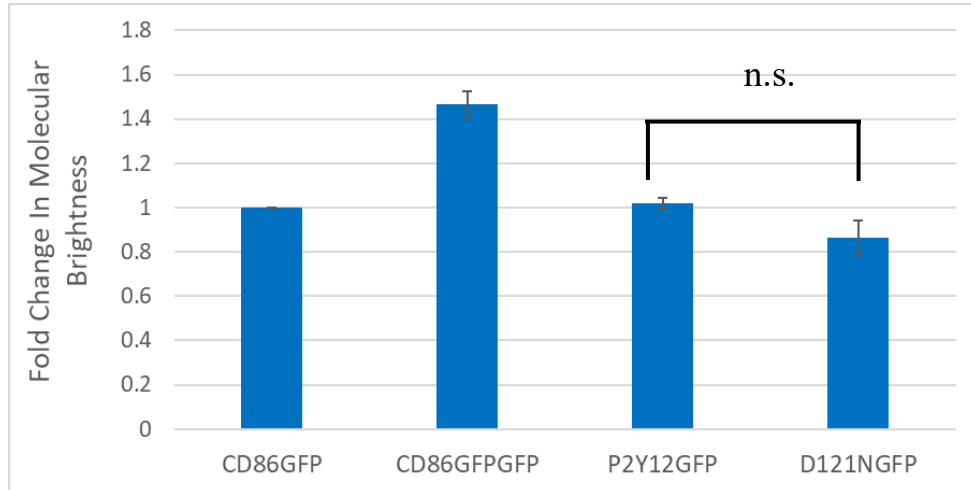


Figure 15: **P2Y12 mutant variant D121N does not form increased homodimers relative to the WT receptor.** HEK293T cells were transiently transfected with CD86-GFP (as a monomeric control), CD86-GFPGFP (as a dimeric control), P2Y12-GFP or P2Y12D121N-GFP and analyzed by FCS and PCH at 36 hours post-transfection. Molecular brightness was measured to determine the oligomeric state of the receptors, which was normalized to the monomeric control (CD86-GFP, set to 1). Presented is the mean of two independent experiments +/- SEM; n.s., not significant, paired student's t-test

3.2.3 P2Y12 Mutant Variant R265W Heterodimerization with PAR4

I next sought to investigate the potential heterodimerization of P2Y12 mutant variants with PAR4. Wild-type P2Y12 directly and functionally associates with PAR4 (Khan *et al* 2014). Untreated R265W/PAR4 co-expressing cells exhibit increased levels of phosphorylated Akt, which may be due to agonist-independent heterodimerization. Additionally, given that an arginine to tryptophan substitution at a.a. 265 alters P2Y12 homodimerization, I was interested in whether it would alter its ability to heterodimerize as well.

In order to investigate P2Y12R265W ability to associate with PAR4, I designed a competition assay using FCS and PCH techniques. HEK293T cells were

transiently transfected with CD86-GFP (monomeric control), CD86-GFPGFP (dimeric control), P2Y12-GFP, or P2Y12R265W-GFP. Additionally, HEK293T cells were transiently co-transfected with P2Y12R265W tagged with GFP and PAR4 tagged with non-fluorescent HA at increasing ratios of 1:1, 1:4, and 1:16. Given that we previously found P2Y12R265W to form increased homodimers, we can investigate its ability to associate with PAR4 by observing if PAR4 can compete out the dimers at increasing concentrations. Since P2Y12R265W is fluorescently tagged with GFP, it will be detected by confocal microscopy, but PAR4 will not. Therefore, if PAR4 is able to compete out the P2Y12R265W dimers, we expect to see a decrease in molecular brightness with increased concentration of PAR4.

Here we find that P2Y12R265W may be able to associate with PAR4. At increasing levels of PAR4, we found a decrease in average molecular brightness in counts per second per molecule (cpsm) from 5962.6 cpsm in cells transfected with P2Y12R265W alone to 4286.4 cpsm in cells co-transfected with P2Y12R265W and PAR4 in a 1:16 ratio which represents nearly a 1.4-fold difference (Figure 16).

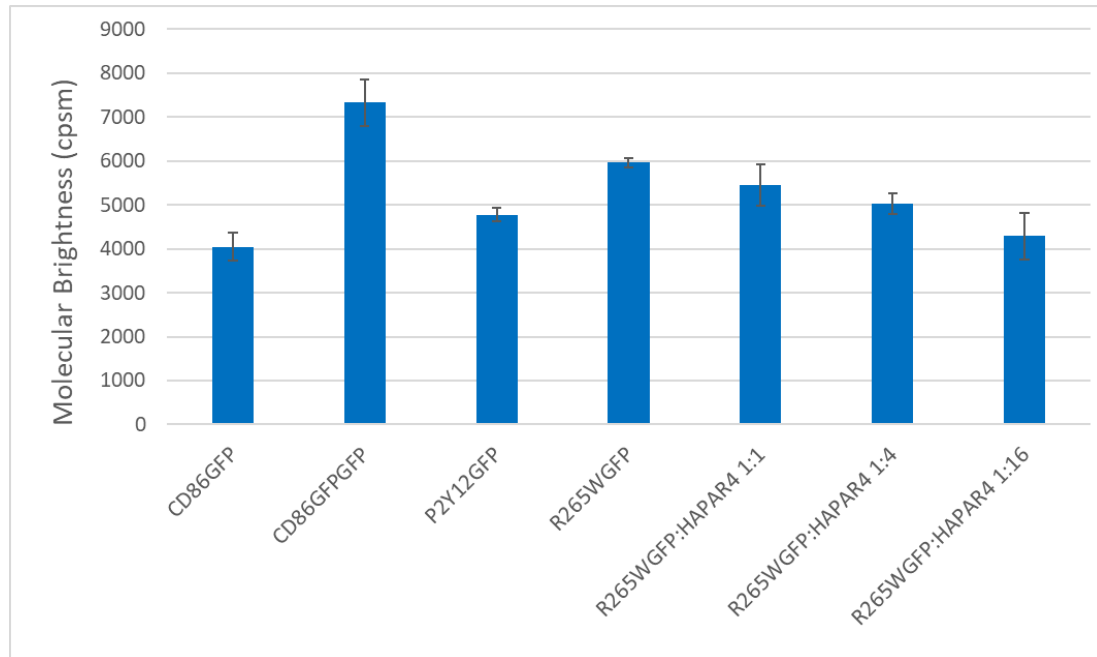


Figure 16: **P2Y12 mutant variant R265W may heterodimerize with PAR4.**

HEK293T cells were transiently transfected with CD86-GFP (monomeric control), CD86-GFPGFP (dimeric control), P2Y12-GFP, and P2Y12 mutant variant R265W-GFP, or co-transfected with P2Y12R265W-GFP and HA-PAR4 in a ratio of 1:1, 1:4, and 1:16. Cells were analyzed by FCS and PCH at 36 hours post transfection. Molecular brightness (in cpsm, counts per second per molecule) was measured to determine the oligomeric state of the receptors. Presented is the mean of 3 to 4 cells +/- SEM from a single experiment.

3.3 G α i Coupling of P2Y12 Mutant Variants R265W and D121N

3.3.1 Background

P2Y12 plays a pivotal role in platelet activation and aggregation (Dorsam & Kunapuli 2004). Activation of P2Y12 results in the inhibition of adenylyl cyclase, lowering cellular levels of cAMP through receptor coupling to G α i (Hecher & Gachet 2011). A patient with congenital bleeding was found to be compound heterozygous for two P2Y12 mutant variants: R256Q and R265W. Platelets isolated from the patient

had a reduced ability to aggregate in response to ADP compared to those from healthy controls. Additionally, these P2Y₁₂ variants appeared to exhibit a G α i defect while agonist-binding and surface expression remained normal (Cattaneo *et al* 2003). This was unexpected as these mutations affect the sixth transmembrane domain (position 256) or third extracellular loop (position 265) of the receptor, as opposed to the cytosolic region where interaction with the G protein occurs.

Previously my lab studied one of these variants, P2Y₁₂R256Q, in isolation in HEK293T cells. In addition to forming increased homodimers relative to WT P2Y₁₂, we found that P2Y₁₂R265Q was unable to lower forskolin-induced cAMP levels (Barnawi 2017). We proposed that increased receptor homodimerization may alter physical association with, or efficient activation of, the heterotrimeric G protein.

In this thesis, I have identified a structural defect in P2Y₁₂ mutant variant R265W, characterized by an increased tendency to homodimerize. Interestingly, this homodimerization defect appeared to be more severe in this variant relative to P2Y₁₂R256Q (Barnawi 2017). Therefore, we predict P2Y₁₂R265W will have a reduced ability to couple G α i.

An individual with no history of bleeding was recently found to be heterozygous for a point mutation D121N, affecting the DRY motif of P2Y₁₂. Platelets isolated from this individual were virtually nonresponsive to ADP and exhibited a severe aggregation defect (Kostyak *et al* 2018). The conserved DRY motif is important for G protein coupling in other class A GPCRs (Nygaard *et al* 2009; Rovati *et al* 2007). I hypothesized that a charge-neutral amino acid substitution affecting the first residue (aspartic acid) of this motif may hinder P2Y₁₂ G α i coupling.

I investigated the ability of P2Y12 mutant variants R265W and D121N to couple to G protein using the GloSensor cAMP assay (Promega). This is a luminescence-based assay, sensitive to detect endogenous levels of cAMP for either kinetic or end-point analysis in living cells. GloSensor technology involves transient transfection of the 20F plasmid construct encoding a mutant form of the firefly luciferase which contains a binding site for cAMP. Analyte binding promotes a conformational change, increasing luminescence activity by a factor directly proportional to the amount of cAMP present in the cells (see Figure 10 in chapter 2, section 2.4.1).

3.3.2 Mutant Variants R265W and D121N are Able to Couple to G α i in a Manner Comparable to Wild-Type P2Y12 in HEK293T Cells

In order to assess the efficiency of receptors to couple G α i, I measured cAMP levels from HEK293T cells mock-transfected with pcDNA compared to those transfected with either wild type P2Y12, or mutant variants R265W or D121N. For each transfection the level of cAMP from untreated cells was subtracted from that of cells treated with adenylyl cyclase activator, forskolin-alone, and from cells treated with forskolin and ADP. Net cAMP levels from forskolin-treated cells were normalized to 100% (forskolin-induced cAMP activity), while levels from cells treated with both forskolin and ADP were taken as a percent of forskolin-induced cAMP activity.

Despite increased homodimerization, I found that P2Y12R265W did not exhibit a G α i coupling defect in our heterologous system, as cells expressing this P2Y12 mutant variant were able to effectively lower cAMP levels in the presence of agonist, ADP. The percent of forskolin-induced cAMP activity was not significantly

different in ADP-treated cells expressing P2Y12R265W when compared to those expressing P2Y12 ($p > 0.05$, unpaired student's t-test). Similarly, we did not find that P2Y12D121N, transiently expressed in HEK293T cells, exhibits a $G_{\alpha i}$ coupling defect. (Figure 17).

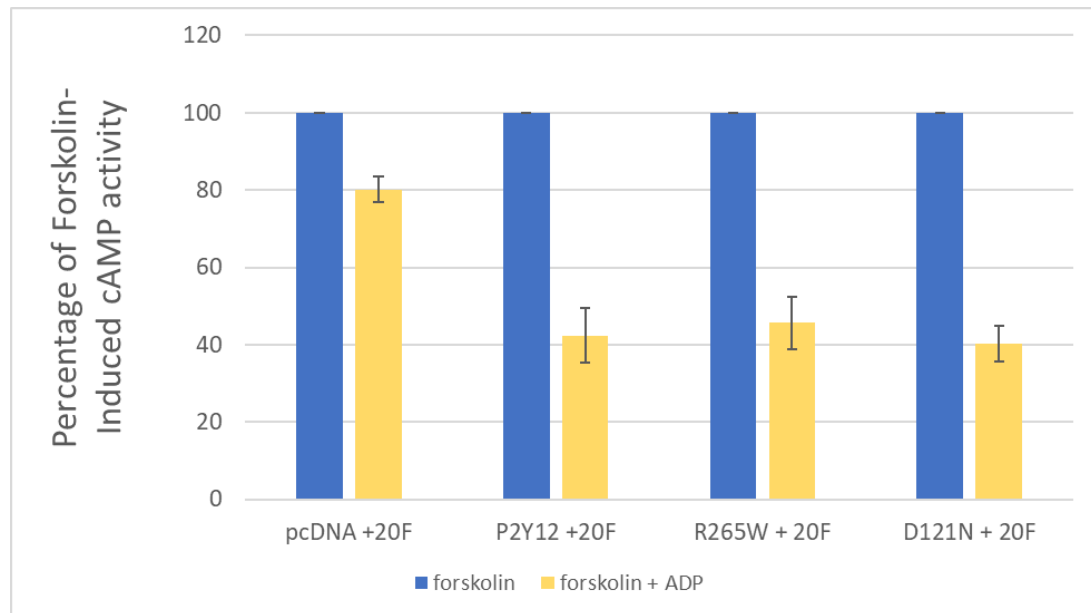


Figure 17: P2Y12 mutant variants R265W and D121N do not show $G_{\alpha i}$ coupling defect in a heterologous expression system. HEK293T cells were transiently co-transfected with pGloSensor-20F cAMP plasmid (20F) along with pcDNA (mock-N=4), P2Y12-GFP (N=4), P2Y12R265W-GFP (N=5), or P2Y12D121N-GFP (N=3). At 36-72 hours post-transfection, cells were lifted, equilibrated in cAMP reagent, and transferred to a 96-well plate. Cells were left untreated or treated with 0.4 μ M forskolin with or without 0.4 μ M ADP. Luminescence was measured to determine the relative levels of cAMP present in the cells. Data was normalized to the percentage of forskolin-induced cAMP activity. Error bars represent SEM.

We were surprised not to find a coupling defect in either P2Y12 mutant variants, particularly R265W which has an increased ability to homodimerize. We proposed that an increase in homodimerization may preclude efficient G α i coupling. Indeed, our lab has previously found a correlation between increased homodimers of another P2Y12 mutant variant, R256Q, and an inability to couple G α i (Barnawi 2017). My results may reflect differences in methodology to this earlier work, but also demonstrate the complexity of GPCR signaling. The possible relationship between receptor dimerization and function needs to be further explored.

While P2Y12D121N did not form increased homodimers relative to WT P2Y12 and was able to couple G α i normally, it promoted increased levels of phosphorylated Akt. We proposed the phenotype exhibited in platelets from the heterozygous individual is the result of desensitization of the receptor due to constitutive activity, affecting responsiveness to ADP.

Chapter 4

DISCUSSION AND FUTURE DIRECTIONS

I characterized two mutant variants of the purinergic platelet receptor, P2Y₁₂, that have been identified in individuals with defective ADP-mediated platelet aggregation (Cattaneo *et al* 2003; Kostyak *et al* 2018). While each mutation is localized in a different region of P2Y₁₂ and may structurally alter the receptor in different ways, both appear to play a role in aberrant signaling. Studying naturally occurring mutant variants provides a better understanding in how they may contribute to symptoms *in vivo*, and alludes to the structure and function of the wild-type receptor.

Despite years of research and newly determined crystal structures (Zhang *et al* 2014a; Zhang *et al* 2014b), the precise contributions of receptor homodimerization and internal molecular interactions governing different active/inactive conformations of P2Y₁₂, remain poorly understood. Our results further demonstrate that mutations resulting in increased dimerization may have negative functional consequences for P2Y₁₂ signaling. Additionally, through investigation of a novel mutant variant affecting the first residue of the DRY motif, we highlighted the significance of this position in regulating receptor activity.

4.1 P2Y₁₂ Mutant Variant R265W

A patient with a mild congenital bleeding disorder was found to be compound heterozygous for two P2Y₁₂ mutant variants, R256Q and R265W, each the result of a

point mutation in the coding region of the P2Y12 gene on separate chromosomes. On platelets isolated from the patient, these variants had normal surface expression and could bind to ADP. However, G α i coupling appeared to be defective (Cattaneo *et al* 2003). This was initially puzzling as G protein association and activation involve the cytosolic regions of the receptor, and these mutations are located in the sixth transmembrane domain (R256Q) or third extracellular loop (R265W) of P2Y12.

Previously, our lab has found that both P2Y12R256Q and P2Y12R265W form increased homodimers relative to WT P2Y12, and found a correlation between P2Y12R256Q homodimerization and a G α i coupling defect (Barnawi 2017). Here we provide further evidence that P2Y12R265W has an increased tendency to homodimerize relative to WT P2Y12, and for the first time, demonstrate its potential to heterodimerize with PAR4. We were surprised to find normal G α i coupling when expressed in isolation, and constitutive activation of Akt when co-expressed with PAR4. The results presented in this thesis, along with those from other studies, demonstrate that P2Y12R265W independently contributes to dysfunctional signaling in platelets that may underly bleeding diathesis.

The increased homodimerization of both P2Y12R256Q and P2Y12R265W in combination with aberrant signaling, support the general consensus that the oligomeric state of class A GPCRs are functionally relevant. Defining functional units, however, has been a challenge met with much controversy, particularly for P2Y12 in which evidence is divided between two working models: 1) P2Y12 is functionally present on cell membranes as a multimeric unit that separates into dimers and monomers when antagonized (Savi *et al* 2006) and 2) P2Y12 is functionally present on cell membranes as a monomer, and dimerization reduces its signaling capabilities (Barnawi 2017). The

first was developed through a biochemical approach using platelet cell lysates. Bands of higher molecular weights than predicted for the P2Y₁₂ monomer were observed on immunoblots, and the intensity of these bands decreased in the presence of the antithrombotic drug, Clopidogrel. These findings may not accurately represent native interactions, however, and do not demonstrate that the reduction in oligomer size was at least partially responsible for P2Y₁₂ antagonism. In contrast, our lab provided compelling evidence that the predominant species of basal P2Y₁₂ in living cells is monomeric through single-molecule confocal techniques, and that P2Y₁₂R256Q when expressed alone, both fails to reduce cellular cAMP levels (G α i defect) and has an increased ability to homodimerize than the wild-type receptor.

Therefore, the findings from our lab are in support of a monomeric P2Y₁₂ where increased homodimerization reduces function. This is in agreement with the antagonist (AZD1283)-bound structure of P2Y₁₂ which was crystalized as a dimer (Zhang *et al* 2014b). However, while homodimerization may reduce membrane stability, and/or prevent either physical association with or activation of heterotrimeric G protein, it may be unrelated to the observed functional deficiencies of P2Y₁₂ mutant variants. For example, while P2Y₁₂R256Q and P2Y₁₂R265W were found to have an increased tendency to homodimerize, monomeric receptors of these variants were still detected that may have functional abnormalities resulting from a global conformational change of the receptor that only coincidentally produces homodimers. Nevertheless, functional consequences of dimerization have been identified in other class A GPCRs, suggesting it may play a role here. For example, homodimerization is important for internalization of the δ opioid receptor (Cvejic & Devi 1997) and

promoting Gαq signaling of PAR4 (Fuente *et al* 2012), but reduces the capacity of NTS1 to activate G protein (White *et al* 2007).

Recently, we found that both P2Y12R256Q and P2Y12R265W have a greater tendency to homodimerize relative to WT P2Y12, and that P2Y12R256Q was inefficient in coupling Gαi, which appeared to be correlated to its increased homodimerization (Barnawi 2017). Because P2Y12R265W appeared to have a homodimerization defect of greater severity than P2Y12R256Q, we expected this mutant variant would also exhibit a Gαi coupling defect. We were therefore surprised to find that P2Y12R265W lowered forskolin-induced cAMP levels comparable to WT P2Y12. While there may be no direct correlation between homodimerization and coupling, a Gαi defect was observed in P2Y12-R256Q/R265W compound heterozygous platelets and two other studies have demonstrated that P2Y12R265W, when expressed in isolation, fails to couple Gαi (Cattaneo *et al* 2003; Mao *et al* 2010). Differences in transfection methodology (stable vs transient), protein tags, and concentrations of both forskolin and ADP, may explain these discrepancies. Interestingly, in both of these studies, P2Y12R265W was able to decrease cAMP levels when treated with high levels of ADP. This suggests that P2Y12R265W retains a degree of functionality that we may be detecting with the conditions used in our study. I cannot rule out the possibility that P2Y12R265W has deficient Gαi coupling *in vivo*.

In this study, we found constitutive activity in P2Y12R265W when co-expressed with PAR4 as the level of phosphorylated Akt was higher than that found in WT P2Y12/PAR4 co expressing cells. Arrestin-mediated Akt activation involves the agonist-induced physical association of P2Y12 and PAR4 (Khan *et al* 2014) and

subsequent internalization (Smith *et al* 2017). An R to W substitution at 265 of P2Y12 may alter the conformation of the receptor such that its heterodimerization with PAR4 is increased in the absence of agonist, resulting in the observed constitutive activation of Akt. In addition, increased homodimerization of P2Y12R265W combined with the observed constitutive activity, may result in receptor desensitization and internalization. While Cattaneo *et al* (2003) did not find a significant difference in the number of ADP binding sites between platelets from the P2Y12-R256Q/R265W compound heterozygote and from healthy individuals, we cannot assume a 1:1 ratio of P2Y12R256Q to P2Y12R265W surface expression, nor rule out the possibility that P2Y12R265W (and/or P2Y12R256Q) participates in altered internalization and recycling. The association of arrestins with GPCRs usually precludes coupling of the heterotrimeric G protein (Luttrell & Gesty-Palmer 2010; Rajagopal & Shenoy 2017). This may be one way that P2Y12R265W contributes to the observed G α i defect in platelets which may in-turn be an underlining cause of the bleeding symptoms in the patient.

4.2 P2Y12 Mutant Variant D121N

A novel point mutation altering amino acid residue aspartic acid (D) 121 to asparagine (N) of the purinergic class A GPCR, P2Y12, resulted in a severe platelet aggregation phenotype in response to ADP (Kostyak *et al* 2018). Our lab became interested in characterizing this novel mutant receptor. I found that this D to N mutation in the first residue of the DRY motif did not affect P2Y12 self-association or G α i coupling, but resulted in increased Akt phosphorylation when co-expressed with another class A GPCR found in human platelets, PAR4.

The DRY motif (or ERY in rhodopsin and several other receptors) is comprised of three amino acid residues Asp^{3.49} (or Glu^{3.49}), Arg^{3.50}, and Trp^{3.51}, where the superscript denotes the Ballesteros–Weinstein “universal” numbering system for class A GPCRs (Ballesteros & Weinstein 1995). In this system, the most conserved residue is denoted “50”, preceded by a decimal point and the transmembrane domain (TM 1-7) in which the residue is located, allowing for direct comparison among different receptors (Isberg *et al* 2015). While GPCRs are diverse and share little homology, the DRY motif, located at the cytosolic end of TM3, is highly conserved. It is thought to be important for regulating receptor conformational states, trafficking, and G protein coupling (Nygaard *et al* 2009).

The involvement of the DRY motif in receptor activation came from the discovery of an “ionic lock” in rhodopsin. The “ionic lock” refers to an interhelical salt bridge between the central arginine (R^{3.50}) of the motif in TM3 and E^{6.30} in TM6. This interaction is broken in its active state, and was originally thought to be a universal mechanism of class A GPCR activation (Hofmann *et al* 2009).

This classical “ionic lock” was not found in all GPCRs. While mutational analysis initially suggested the presence of an ionic lock in β 2AR (Ballesteros *et al* 2001), crystal structures were not in agreement (Cherezov *et al* 2007; Rosenbaum *et al* 2007). Other class A GPCRs, such as β 1AR and adenosine A2A receptor, were also found to lack an ionic lock suggesting this cannot be a general feature of these receptors (Hanson & Stevens 2009). Interestingly, receptors lacking this ionic lock tend to have varying degrees of constitutive activity. However, their activity is increased in the presence of agonists suggesting that other interactions are present in the basal state, preventing full activation. It was found that R^{3.50} forms another

intrahelical polar interaction with the adjacent D^{3.49} of the DRY motif in the inactive “dark state” of rhodopsin (Vogel *et al* 2008), which appears to be more conserved than the interaction between TM3 and TM6 (Rovati *et al* 2017). Furthermore, this interaction was characterized as being stronger and more critical than the R^{3.50}-E^{6.30} salt bridge in dark state rhodopsin, highlighting another key interaction maintaining receptor inactivation (Vogel *et al* 2008).

Crystal structure of P2Y12 revealed that it does not form an ionic lock as the R^{3.50} was positioned in plane with a hydrophobic V^{6.37} instead of the prototypical E^{6.30} found in rhodopsin (Zhang *et al* 2014b). While this may explain the reported basal activity of this receptor (Aungraheeta *et al* 2016), it also highlights the possibility that D^{3.49} plays a prime role in modulating receptor activity.

The importance of D^{3.49} in receptor activation/inactivation has been further demonstrated by mutational analysis of several GPCRs (Rovati *et al* 2007). In the highly studied β 2AR, a D^{3.49} to N mutation resulted in increased cAMP levels (G α s activity) in the absence of ligand in when heterologously expressed in COS7 cells (Ballesteros *et al* 2001). Furthermore, Kaposi’s sarcoma-associated herpesvirus (KSHV) encodes a GPCR containing a V^{3.49}R^Y motif that exhibits constitutive activity promoting uncontrolled cellular proliferation (Leandros *et al* 1997). Therefore, the charge-neutralizing D^{3.49} to N mutation in position 121 of P2Y12 may preclude normal residue interactions controlling the basal state of the receptor, and explain the increased levels of phosphorylated Akt in P2Y12D121N-expressing cells in the absence of ADP. Furthermore, the central R^{3.50} of the DRY motif, which is not affected in our P2Y12-D121N mutant, may be more important for G protein coupling (Rovati *et al* 2007), which may explain why we did not observe a G α i defect.

If P2Y₁₂ mutant variant D121N demonstrates normal agonist-dependent G α i coupling, how might it mediate dysfunctional ADP-dependent platelet aggregation? Based on the results we obtained from the cAMP assay, it appears that P2Y₁₂D121N has the capability to interact normally with agonist and transduce signals. We therefore propose that the platelets from the P2Y₁₂D121N heterozygous patient are nonresponsive to ADP as a result of desensitization due to constitutive Akt activation. P2Y₁₂D121N may contribute to agonist-independent Akt activation through heterodimerization with PAR4, which will be addressed in future work.

P2Y₁₂ is normally desensitized following prolonged agonist stimulation through phosphorylation on key cytosolic residues by G protein-coupled receptor kinase 2 (GRK2) and GRK6. This promotes association with arrestin-2 (β -arrestin) and subsequent internalization through clathrin-mediated endocytosis, thereby reducing the responsiveness of cells to ADP. P2Y₁₂ is rapidly recycled to the plasma membrane where it can participate in another wave of signaling events (Mundell *et al* 2006). Mutations in GPCRs resulting in agonist-independent desensitization may reduce cell responsiveness to a particular agonist, either by increasing the frequency of internalization or by aberrant intracellular trafficking that slows or prevents recycling.

A naturally-occurring mutant variant of human vasopressin type II receptor (V2R) in which the central R^{3.50} of the DRY motif is substituted with histidine, (R137H) exhibits constitutive desensitization through β -arrestin recruitment and internalization in the absence of agonist (Barak *et al* 2001). This V2R mutant has been shown to influence agonist-independent internalization of another vasopressin receptor, V1aR through heterodimerization. Furthermore, V1aR was not rapidly recycled to the membrane as is typical when expressed independently (Terrillon *et al*

2004). A similar mechanism may explain why platelets from an individual, heterozygous for P2Y₁₂ mutant variant D121N, have a severe aggregation defect. While P2Y₁₂D121N appears to be predominantly monomeric similar to that of WT P2Y₁₂ in live HEK 293T cells, it may interact with the wild-type receptor influencing its presence on the plasma membrane and ability to respond to ADP.

Interestingly another DRY motif variant has been reported for P2Y₁₂ resulting in a R^{3.50} to C substitution (R122C). Platelet surface expression of this variant (from a patient with a lifelong history of bleeding who was homozygous for P2Y₁₂R122C), is lower than surface expression of P2Y₁₂ on platelets from healthy controls. When expressed heterologously in human astrocytoma 1321N1 cells, P2Y₁₂R122C was internalized more rapidly than WT P2Y₁₂ in the absence of agonist. Furthermore, the mutant receptor showed higher co-localization with a lysosomal marker and lower co-localization with transferrin (marker for recycling endosomes) compared to WT P2Y₁₂ (Patel *et al* 2014). Similarly, P2Y₁₂D121N may be internalized and preferentially trafficked to lysosomes for degradation than recycled to the membrane. It would be of interest to perform similar co-localization studies on P2Y₁₂D121N to further understand how this receptor influences deficient ADP-dependent platelet aggregation.

4.3 Summary of Conclusions

P2Y₁₂, the target of clinically effective antithrombotic drugs such as Clopidogrel, is a class A GPCR that mediates platelet activation and aggregation. Naturally occurring mutations have been found in P2Y₁₂ that affect platelet aggregation and may explain bleeding phenotypes in patients. P2Y₁₂ variant R265W was identified in a patient with congenital bleeding who was compound heterozygous

for both this variant and another, R256Q (Cattaneo *et al* 2003). A second individual with a severe defect in ADP-mediated platelet aggregation was found to be heterozygous for a mutation in the DRY motif of P2Y₁₂, resulting in an aspartic acid to asparagine substitution at 121 (D121N). This severity was unanticipated as they express wild type receptor that should compensate for the D121N variant (Kostyak *et al* 2018).

Here I found that P2Y₁₂ mutant variants R265W and D121N, when co-expressed with PAR4, promote increased activation of Akt in the absence of either P2Y₁₂ agonist ADP or PAR4 agonist AYPGKF. We proposed this may be the result of synergy with PAR4. Consistent with this hypothesis, we found that P2Y₁₂R265W may heterodimerize with PAR4. Additionally, we found an increased tendency to homodimerize relative to the wild-type receptor in P2Y₁₂R265W, but not P2Y₁₂D121N. It has yet to be investigated whether P2Y₁₂D121N dimerizes with wild-type P2Y₁₂ to preclude its normal functioning, which may explain the apparent dominant-negative phenotype in the patient. We expected to find a correlation between increased dimerization of P2Y₁₂R265W and G α i coupling as was previously found for another P2Y₁₂ mutant variant, R256Q (Barnawi 2017). Interestingly, we found that neither P2Y₁₂R265W nor P2Y₁₂D121N were deficient in coupling to G α i.

Previous studies suggest that P2Y₁₂R265W independently contributes to the G α i coupling defect seen in the P2Y₁₂-R256Q/R265W compound heterozygous platelets. However, it was determined that the receptor is not entirely nonfunctional (Cattaneo *et al* 2003; Mao *et al* 2010). Therefore, it is possible that our experimental system may have enabled normal G α i coupling that may not be present physiologically. Alternatively, the relationship between receptor dimerization and

coupling may not be directly correlated. P2Y₁₂D121N may contribute to aberrant ADP-dependent platelet aggregation through desensitization as a result of constitutive activity which would reduce platelet responsiveness to subsequent ADP exposure. This is supported through work from other laboratories linking the DRY motif to controlling receptor conformational states affecting their level of activity (Ballesteros *et al* 2001; Favre *et al* 2005; Rovati *et al* 2007).

4.4 Future Directions

4.4.1 Investigate Dimeric Potential of P2Y₁₂ Mutant Variant D121N with Wild-Type Receptor

A point mutation resulting in an amino acid substitution of aspartic acid (D) to asparagine (N) at position 121 of P2Y₁₂ was found in an individual with no history of bleeding. While this individual was heterozygous for this mutant, their platelets had a severe aggregation defect that was unanticipated (Kostyak *et al* 2018). We expect reduced severity in heterozygotes because the expressed wild-type receptor should be able, at least partially, to compensate. Instead, it appears the D121N mutant variant acts in a dominant negative manner. We propose P2Y₁₂D121N may physically interact with the wild type receptor, precluding its function. Although we found that P2Y₁₂D121N does not form increased homodimers relative to the degree of self-association of the wild-type receptor, we have not yet investigated the possibility that it may dimerize with WT P2Y₁₂. It is possible that this mutation alters receptor conformation discouraging self-association, but maintaining an interface that allows for interaction with the wild-type receptor. We plan to investigate this possibility using bioluminescence resonance energy transfer (BRET). This technique allows for the detection of protein-protein interactions through proximity of an energy donor (Renilla

luciferase (Rluc)) and acceptor (YFP). The acceptor becomes excited at the emitted wavelength of the donor, in-turn emitting light at a unique wavelength. Our lab currently has the Rluc donor-tagged WT P2Y12 construct, and I have recently created a construct containing P2Y12 mutant variant D121N fused to the YFP acceptor tag.

4.4.2 Determine the Ability of P2Y12 Mutant Variants to Heterodimerize to PAR4 Relative to That of WT P2Y12

Wild-type P2Y12 has been found to physically associate with PAR4 in a functionally relevant manner, mediating the activation of Akt (Khan *et al* 2014). Here, I have demonstrated that P2Y12 mutant variant R265W, originally identified in a patient with congenital bleeding (Cattaneo *et al* 2003), may heterodimerize with PAR4. However, it is not clear whether these dimeric tendencies are increased relative to that of the WT P2Y12 receptor or how the P2Y12R265W-PAR4 heterodimer might be influenced by agonists. Furthermore, we have not yet investigated the heteromeric potential of other P2Y12 mutant variants currently being studied in our lab (R256Q and D121N). Interestingly, both P2Y12R265W and P2Y12D121N appear to have constitutive activity in mediating Akt phosphorylation. Compared to WT P2Y12, I hypothesize that both P2Y12R265W and P2Y12D121N form increased heterodimers with PAR4 in the absence of agonists. We plan to use the available constructs in my lab, containing Rluc-tagged WT or mutant P2Y12, and YFP-tagged PAR4, to develop a BRET assay.

4.4.3 Arrestin-2 Recruitment to P2Y12 Mutant Variants and PAR4

Synergy between P2Y12 and PAR4, and the recruitment of arrestin-2 to the P2Y12-PAR4 heterodimer, is important for maximal Akt activation. Arrestin recruitment to PAR4 only occurs when co-expressed with P2Y12 and is increased in

the presence of PAR4 agonist AYPGKF (Khan *et al* 2014). Given that P2Y12 mutant variants R265W and D121N when co-expressed heterologously with PAR4 in HE293T cells exhibit constitutive activation of Akt, they may efficiently recruit arrestin-2 in the absence of agonists. Furthermore, both the heterodimerization tendencies of PAR4 and P2Y12, and the degree of co-immunoprecipitation of arrestin-2 and PAR4, decrease in the presence of P2Y12 antagonist, MeSAMP. Mao *et al* (2010) found that the R265W mutation in P2Y12 increases sensitivity to P2Y12 antagonist AR-C69931MX. It would be interesting to see how arrestin recruitment to constitutively active P2Y12 mutant receptors is influenced by antagonism. This can be investigated through co-immunoprecipitation of P2Y12 and PAR4 with arrestin-2 or through BRET analysis.

REFERENCES

- Abbracchio, M. P., Burnstock, G., Boeynaems, J. M., Barnard, E. A., Boyer, J. L., Kennedy, C., . . . Weisman, G. A. (2006). International Union of Pharmacology LVIII: update on the P2Y G protein-coupled nucleotide receptors: from molecular mechanisms and pathophysiology to therapy. *Pharmacological Reviews*, 58(3), 281-341.
- Angers, S., Salahpour, A., Joly, E., Hilairet, S., Chelsky, D., Dennis, M., & Bouvier, M. (2000). Detection of β 2 -adrenergic receptor dimerization in living cells using bioluminescence resonance energy transfer (BRET). *PNAS*, 97(7), 3684–3689.
- Arachiche, A., Mumaw, M. M., Fuente, M. d. l., & Nieman, M. T. (2013). Protease-activated Receptor 1 (PAR1) and PAR4 Heterodimers Are Required for PAR1-enhanced Cleavage of PAR4 by α -Thrombin. *Journal of Biological Chemistry*, 288, 32553-32562
- Arvanitakis, L., Geras-Raaka, E., Varma, A., Gershengorn, M. C., & Cesarman, E. (1997). Human herpesvirus KSHV encodes a constitutively active G-protein-coupled receptor linked to cell proliferation. *Nature*, 385(6614), 347-350.
- Aungraheeta, R., Conibear, A., Butler, M., Kelly, E., Nylander, S., Mumford, A., & Mundell, S. J. (2016). Inverse agonism at the P2Y12 receptor and ENT1 transporter blockade contribute to platelet inhibition by ticagrelor. *Blood*, 128(23), 2717–2728.
- Bacia, K., Kim, S. A., & Schwille, P. (2006). Fluorescence cross-correlation spectroscopy in living cells. *Nature Methods*, 3(2), 83-89.
- Ballesteros, J. A., Jensen, A. D., Liapakis, G., Rasmussen, S. G. F., Shi, L., Gether, U., & Javitch, J. A. (2001). Activation of the β ₂-Adrenergic Receptor Involves Disruption of an Ionic Lock between the Cytoplasmic Ends of Transmembrane Segments 3 and 6. *Journal of Biological Chemistry*, 276, 29171-29177.
- Ballesteros, J. A., & Weinstein, H. (1995). Integrated methods for the construction of three-dimensional models and computational probing of structure-function relations in G protein-coupled receptors. *Methods in Neurosciences*, 25, 366-428.

- Barak, L. S., Oakley, R. H., Laporte, S. A., & Caron, M. G. (2001). Constitutive arrestin-mediated desensitization of a human vasopressin receptor mutant associated with nephrogenic diabetes insipidus. *PNAS*, 98(1), 93-98.
- Barnawi, F. (2017). *Functional analysis of the dimerization potential of the P2Y12 receptor and two naturally-occurring mutant variants*. (Master of Science). University of Delaware, Retrieved from <http://udspace.udel.edu/handle/19716/23544> (1038067308)
- Barthet, G., Carrat, G., Cassier, E., Barker, B., Gaven, F., Pillot, M., . . . Dumuis, A. (2009). beta-arrestin1 phosphorylation by GRK5 regulates G protein-independent 5-HT4 receptor signalling. *The EMBO Journal*, 28, 2706–2718.
- Bayburt, T. H., Leitz, A. J., Xie, G., Oprian, D. D., & Sligar, S. G. (2007). Transducin Activation by Nanoscale Lipid Bilayers Containing One and Two Rhodopsins. *Journal of Biological Chemistry*, 282, 14875-14881.
- Briddon, S. J., & Hill, S. J. (2007). Pharmacology under the microscope: the use of fluorescence correlation spectroscopy to determine the properties of ligand–receptor complexes. *Trends in Pharmacological Sciences*, 28(12), 637-645.
- Capra, V., Mauri, M., Guzzi, F., Busnelli, M., Accomazzo, M. R., Gaussem, P., . . . Rovati, G. E. (2017). Impaired thromboxane receptor dimerization reduces signaling efficiency: A potential mechanism for reduced platelet function in vivo. *Biochemical Pharmacology*, 24, 43-56.
- Cattaneo, M. (2008). Advances in antiplatelet therapy: overview of new P2Y12 receptor antagonists in development. *European Heart Journal Supplements*, 10, I33–I37.
- Cattaneo, M., Zighetti, M. L., Lombardi, R., Martinez, C., Lecchi, A., Conley, P. B., . . . Ruggeri, Z. M. (2003). Molecular bases of defective signal transduction in the platelet P2Y 12 receptor of a patient with congenital bleeding. *Proceedings of the National Academy of Sciences of the United States of America*, 100(4), 1978–1983.
- Chen, J., De, S., Damron, D. S., Chen, W. S., Hay, N., & Byzova, T. V. (2004). Impaired platelet responses to thrombin and collagen in AKT-1—deficient mice. *Blood*, 104(6), 1703–1710.
- Chen, Y., Muller, J. D., So, P. T. C., & Gratton, E. (1999). The Photon Counting Histogram in Fluorescence Fluctuation Spectroscopy. *Biophysical Journal*, 77, 553-567.

- Cherezov, V., Rosenbaum, D. M., Hanson, M. A., Rasmussen, S. G. F., Thian, F. S., Kobilka, T. S., . . . Stevens, R. C. (2007). High-Resolution Crystal Structure of an Engineered Human beta2-Adrenergic G Protein-Coupled Receptor. *Science*, *318*(5854), 1258-1265
- Coughlin, S. R. (2005). Protease-activated receptors in hemostasis, thrombosis and vascular biology. *Journal of Thrombosis and Haemostasis*, *3*(8), 1800-1814.
- Cunningham, M. R., Nisar, S. P., & Mundell, S. J. (2013). Molecular mechanisms of platelet P2Y12 receptor regulation. *Biochemical Society Transactions*, *41*, 225–230
- Cvejic, S., & Devi, L. A. (1997). Dimerization of the δ Opioid Receptor: Implication for a Role in Receptor Internalization. *Journal of Biological Chemistry*, *272*, 26959-26964.
- DeWire, S. M., Ahn, S., Lefkowitz, R. J., & Shenoy, S. K. (2007). β -Arrestins and Cell Signaling. *Annual Review of Physiology*, *69*, 483–510.
- Dorsam, R. T., & Kunapuli, S. P. (2004). Central role of the P2Y12 receptor in platelet activation. *Journal of Clinical Investigation*, *113*(3), 340–345.
- Fan, F., Binkowski, B. F., Butler, B. L., Stecha, P. F., Lewis, M. K., & Wood, K. V. (2008). Novel Genetically Encoded Biosensors Using Firefly Luciferase. *ACS Chemical Biology*, *3*(6), 346-351.
- Fanelli, F., Mauri, M., Capra, V., Raimondi, F., Guzzi, F., Ambrosio, M., . . . Parenti, M. (2011). Light on the structure of thromboxane A2 receptor heterodimers. *Cellular and Molecular Life Sciences*, *68*(18), 3109–3120.
- Favre, N., Fanelli, F., Missotten, M., Nichols, A., Wilson, J., di Tiani, M., . . . Scheer, A. (2005). The DRY Motif as a Molecular Switch of the Human Oxytocin Receptor. *Biochemistry*, *44*(30), 9990-10008.
- Ferguson, S. S. G. (2007). Phosphorylation-independent attenuation of GPCR signaling. *Trends in Pharmacological Sciences*, *28*(4), 173-179.
- Fuente, M. d. l., Noble, D. N., Verma, S., & Nieman, M. T. (2012). Mapping Human Protease-activated Receptor 4 (PAR4) Homodimer Interface to Transmembrane Helix 4. *Journal of Biological Chemistry*, *287*, 10414-10423.

- Gao, Y., Westfield, G., Erickson, J. W., Cerione, R. A., Skiniotis, G., & Ramachandran, S. (2017). Isolation and structure–function characterization of a signaling-active rhodopsin–G protein complex. *Journal of Biological Chemistry*, *292*, 14280-14289
- Ghoshal, K., & Bhattacharyya, M. (2014). Overview of Platelet Physiology: Its Hemostatic and Nonhemostatic Role in Disease Pathogenesis. *The Scientific World Journal*.
- Guidetti, G. F., Canobbio, I., & Torti, M. (2015). PI3K/Akt in platelet integrin signaling and implications in thrombosis. *Advances in Biological Regulation*, *59*, 36-52.
- Guo, W., Shi, L., Filizola, M., Weinstein, H., & Javitch, J. A. (2005). Crosstalk in G protein-coupled receptors: Changes at the transmembrane homodimer interface determine activation. *PNAS*, *102*(48), 17495-17500.
- Gurevich, V. V., & Gurevich, E. V. (2008). How and why do GPCRs dimerize? *Trends in Pharmacological Sciences*, *29*(5), 234-240.
- Gurevich, V. V., & Gurevich, E. V. (2018). GPCRs and Signal Transducers: Interaction Stoichiometry. *Trends in Pharmacological Sciences*, *39*(7), 672-684.
- Hague, C., Uberti, M. A., Chen, Z., Bush, C. F., Jones, S. V., Ressler, K. J., . . . Minneman, K. P. (2004). Olfactory receptor surface expression is driven by association with the β 2 -adrenergic receptor. *PNAS*, *101*(37), 13672-13676.
- Hanson, M. A., & Stevens, R. C. (2009). Discovery of New GPCR biology – One Receptor Structure at a Time. *Structure*, *17*(1).
- Hechler, B., & Gachet, C. (2011). P2 receptors and platelet function. *Purinergic Signaling*, *7*(3), 293–303.
- Herrick-Davis, K., Grinde, E., Cowan, A., & Mazurkiewicz, J. E. (2013). Fluorescence Correlation Spectroscopy Analysis of Serotonin, Adrenergic, Muscarinic, and Dopamine Receptor Dimerization: The Oligomer Number Puzzle. *Molecular Pharmacology*, *84*(4).
- Herrick-Davis, K., Grinde, E., Lindsley, T., Cowan, A., & Mazurkiewicz, J. E. (2012). Oligomer Size of the Serotonin 5-Hydroxytryptamine 2C (5-HT_{2C}) Receptor Revealed by Fluorescence Correlation Spectroscopy with Photon Counting Histogram Analysis: Evidence for Homodimers Without Monomers or Tetramers. *Journal of Biological Chemistry*, *287*, 23604-23614.

- Herrick-Davis, K., Grinde, E., Lindsley, T., Teitler, M., Mancina, F., Cowan, A., & Mazurkiewicz, J. E. (2015). Native Serotonin 5-HT_{2C} Receptors Are Expressed as Homodimers on the Apical Surface of Choroid Plexus Epithelial Cells. *Molecular Pharmacology*, *87*(4), 660–673.
- Hilger, D., Masureel, M., & Kobilka, B. K. (2018). Structure and dynamics of GPCR signaling complexes. *Nature Structural & Molecular Biology*, *25*, 4-12.
- Hofmann, K. P., Scheerer, P., Hildebrand, P. W., Choe, H.-W., Park, J. H., Heck, M., & Ernst, O. P. (2009). A G protein-coupled receptor at work: the rhodopsin model. *Trends in Biochemical Sciences*, *34*(11), 540-552.
- Holinstat, M., Voss, B., Bilodeau, M. L., McLaughli, J. N., Cleato, J., & Ham, H. E. (2006). PAR4, but Not PAR1, Signals Human Platelet Aggregation via Ca²⁺ Mobilization and Synergistic P2Y₁₂ Receptor Activation. *Journal of Biological Chemistry*, *281*, 26665-26674.
- Hou, Y., Carrim, N., Wang, Y., Gallant, R. C., Marshall, A., & Ni, H. (2015). Platelets in hemostasis and thrombosis: Novel mechanisms of fibrinogen-independent platelet aggregation and fibronectin-mediated protein wave of hemostasis. *Journal of Biomedical Research*, *29*(6), 437-444.
- Irannejad, R., & Zastrow, M. v. (2014). GPCR signaling along the endocytic pathway. *Current Opinion in Cell Biology*, *27*, 109-116.
- Isberg, V., de Graaf, C., Bortolato, A., Cherezov, V., Katritch, V., Marshall, F. H., . . . Gloriam, D. E. (2015). Generic GPCR Residue Numbers - Aligning Topology Maps Minding the Gaps. *Trends in Pharmacological Sciences*, *36*(1), 22-31.
- Jastrzebska, B., Fotiadis, D., Jang, G.-F., Stenkamp, R. E., Engel, A., & Palczewski, K. (2006). Functional and Structural Characterization of Rhodopsin Oligomers. *Journal of Biological Chemistry*, *281*(17), 11917–11922.
- Kahner, B. N., Shankar, H., Murugappan, S., Prasad, G. L., & Kunapuli, S. P. (2006). Nucleotide receptor signaling in platelets. *Journal of Thrombosis and Haemostasis*, *4*(11), 2317-2326.
- Kaupmann, K., Malitschek, B., Schuler, V., Heid, J., Froestl, W., Beck, P., . . . Bettler, B. (1998). GABA B₁-receptor subtypes assemble into functional heteromeric complexes. *Nature*, *396*, 683 – 687.
- Kelly, E., Bailey, C. P., & Henderson, G. (2007). Agonist-selective mechanisms of GPCR desensitization. *British Journal of Pharmacology*, *153*, S379–S388.

- Kerppola, T. K. (2008). Bimolecular fluorescence complementation (BiFC) analysis as a probe of protein interactions in living cells. *Annual Review of Biophysics*, 37, 465–487.
- Khan, A. (2015). *Structural and functional interactions of platelet thrombin and ADP receptors*. (Doctor of Philosophy). University of Delaware, Retrieved from <http://udspace.udel.edu/handle/19716/17599> (946311459)
- Khan, A., Li, D., Ibrahim, S., Smyth, E., & Woulfe, D. S. (2014). The Physical Association of the P2Y₁₂ Receptor with PAR4 Regulates Arrestin-Mediated Akt Activation. *Molecular Pharmacology*, 86(1), 1-11.
- Kilpatrick, L. E., & Hill, S. J. (2016). The use of fluorescence correlation spectroscopy to characterize the molecular mobility of fluorescently labelled G protein-coupled receptors. *Biochemical Society Transactions*, 44(22), 624-629.
- Kim, S., Foster, C., Lecchi, A., Quinton, T. M., Prosser, D. M., Jin, J., . . . Kunapuli, S. P. (2002). Protease-activated receptors 1 and 4 do not stimulate G_i signaling pathways in the absence of secreted ADP and cause human platelet aggregation independently of G_i signaling. *Blood*, 99, 3629-3636.
- Kim, S., Jin, J., & Kunapuli, S. P. (2006). Relative contribution of G-protein-coupled pathways to protease-activated receptor-mediated Akt phosphorylation in platelets. *Blood* 107, 947-954.
- Kostyak, J. C., Dangelmaier, C. A., Mauri, B. R., Patel, A., & Kunapuli, S. P. (2018). Severely Impaired Platelet Function Due to a Novel Mutation of P2Y₁₂ from a Human Subject with No History of Bleeding. *Blood*, 132, 1130.
- Kroeze, W. K., Sheffler, D. J., & Roth, B. L. (2003). G-protein-coupled receptors at a glance. *Journal of Cell Science*, 116, 4867-4869.
- Lai, H.-T., & Chiang, C.-M. (2013). Bimolecular Fluorescence Complementation (BiFC) Assay for Direct Visualization of Protein-Protein Interaction *in vivo*. *BioProtocol*, 3(20), e935.
- Lavoie, C., Mercier, J.-F., Salahpour, A., Umapathy, D., Breit, A., Villeneuve, L.-R., . . . Hébert, T. E. (2002). β_1/β_2 -Adrenergic Receptor Heterodimerization Regulates β_2 -Adrenergic Receptor Internalization and ERK Signaling Efficacy. *Journal of Biological Chemistry*, 277, 35402-35410
- Lee, S.-M., Booe, J. M., & Pioszak, A. A. (2015). Structural insights into ligand recognition and selectivity for class A, B, and C GPCRs. *European Journal of Pharmacology*, 763, 196-205.

- Li, D., D'Angelo, L., Chavez, M., & Woulfe, D. S. (2011). Arrestin-2 Differentially Regulates PAR4 and ADP Receptor Signaling in Platelets. *Journal of Biological Chemistry*, 286(5), 3805–3814.
- Li, J., Ning, Y., Hedley, W., Saunders, B., Chen, Y., Tindill, N., . . . Subramaniam, S. (2002). The Molecule Pages database. *Nature*, 420, 716-717.
- Li, Z., Delaney, M. K., O'Brien, K. A., & Du, X. (2010). Signaling during platelet adhesion and activation. *Arteriosclerosis, Thrombosis, and Vascular Biology*, 30(12), 2341–2349.
- Liang, Y., Fotiadis, D., Filipek, S., Saperstein, D. A., Palczewski, K., & Engel, A. (2003). Organization of the G Protein-coupled Receptors Rhodopsin and Opsin in Native Membranes. *Journal of Biological Chemistry*, 278(24), 21655–21662.
- Lisman, T., Weeterings, C., & de Groot, P. G. (2005). Platelet aggregation: involvement of thrombin and fibrin(ogen). *Frontiers in Bioscience*, 10, 2504-2517
- Lohse, M. J., Nuber, S., & Hoffmann, C. (2012). Fluorescence/Bioluminescence Resonance Energy Transfer Techniques to Study G-Protein-Coupled Receptor Activation and Signaling. *Pharmacological Reviews*, 64(2), 299-336.
- Luttrell, L. M., & Gesty-Palmer, D. (2010). Beyond Desensitization: Physiological Relevance of Arrestin-Dependent Signaling. *PHARMACOLOGICAL REVIEWS*, 62(2), 305–330.
- Mao, Y., Zhang, L., Jin, J., Ashby, B., & Kunapuli, P. S. (2010). Mutational analysis of residues important for ligand interaction with the human P2Y12 receptor. *European Journal of Pharmacology*, 644(1-3), 10–16.
- Milligan, G. (2008). G protein-coupled receptor dimerisation: Molecular basis and relevance to function. *British Journal of Pharmacology*, 153(1), 825-838.
- Mundell, S. J., Luo, J., Benovic, J. L., Conley, P. B., & Poole, A. W. (2006). Distinct Clathrin-Coated Pits Sort Different G Protein-Coupled Receptor Cargo. *Traffic*, 7, 1420–1431.
- Nygaard, R., Frimurer, T. M., Holst, B., Rosenkilde, M. M., & Schwartz, T. W. (2009). Ligand binding and micro-switches in 7TM receptor structures. *Trends in Pharmacological Sciences*, 30(5), 249-259.

- Offermanns, S. (2006). Activation of platelet function through G protein-coupled receptors. *Circulation Research*, 99(12), 1293-1304.
- Patel, Y. M., Lordkipanidzé, M., Lowe, G. C., Nisar, S. P., Garner, K., Stockley, J., . . . Mundell, S. J. (2014). A novel mutation in the P2Y₁₂ receptor and a function-reducing polymorphism in protease-activated receptor 1 in a patient with chronic bleeding. *Journal of Thrombosis and Haemostasis*, 12(5), 716-725.
- Penn, R. B., & Benovic, J. L. (2008). Regulation of Heterotrimeric G Protein Signaling in Airway Smooth Muscle. *Proceedings of the American Thoracic Society*, 5(1).
- Petersen, J., Wright, S. C., Rodríguez, D., Matricon, P., Lahav, N., Vromen, A., . . . Schulte, G. (2017). Agonist-induced dimer dissociation as a macromolecular step in G protein-coupled receptor signaling. *Nature Communications*, 8.
- Rajagopal, S., & Sheno, S. K. (2017). GPCR Desensitization: Acute and Prolonged Phases. *Cell Signal*, 41, 9–16.
- Rasmussen, S. G., DeVree, B. T., Zou, Y., Kruse, A. C., Chung, K. Y., Kobilka, T. S., . . . Kobilka, B. K. (2011). Crystal structure of the β ₂ adrenergic receptor-Gs protein complex. *Nature*, 477(7366), 549-555.
- Rosenbaum, D. M., Cherezov, V., Hanson, M. A., Rasmussen, S. G. F., Thian, F. S., Kobilka, T. S., . . . Kobilka, B. K. (2007). GPCR Engineering Yields High-Resolution Structural Insights into β 2 -Adrenergic Receptor Function. *Science*, 318(5854), 1266-1273.
- Rosenbaum, D. M., Rasmussen, S. G. F., & Kobilka, B. K. (2009). The structure and function of G-protein-coupled receptors. *Nature*, 495(7245), 356-363.
- Rovati, G. E., Capra, V., & Neubig, R. R. (2007). The Highly Conserved DRY Motif of Class A G Protein-Coupled Receptors: Beyond the Ground State. *Molecular Pharmacology*, 71, 959–964.
- Rovati, G. E., Capra, V., Shaw, V. S., Malik, R. U., Sivaramakrishnan, S., & Neubig, R. R. (2017). The DRY motif and the four corners of the cubic ternary complex model. *Cellular Signalling*, 35, 16-23
- Salahpour, A., Angers, S., Mercier, J.-F., Lagace, M., Marullo, S., & Bouvier, M. (2004). Homodimerization of the beta₂-Adrenergic Receptor as a Prerequisite for Cell Surface Targeting. *Journal of Biological Chemistry*, 279(32), 33390–33397.

- Sambu, N., & Curzen, N. (2011). Monitoring the effectiveness of antiplatelet therapy: opportunities and limitations. *British Journal of Clinical Pharmacology*, 72(4), 683–696.
- Savi, P., Zacharyus, J.-L., Delesque-Touchard, N., Labouret, C., Hervé, C., Uzabiaga, M.-F., . . . Herbert, J.-M. (2006). The active metabolite of Clopidogrel disrupts P2Y₁₂ receptor oligomers and partitions them out of lipid rafts. *PNAS*, 103(29), 11069-11074.
- Siderovski, D. P., & Willard, F. S. (2005). The GAPs, GEFs, and GDIs of heterotrimeric G-protein alpha subunits. *International Journal of Biological Sciences*, 1(2), 51-66.
- Smith, T. H., Li, J. G., Dores, M. R., & Trejo, J. (2017). Protease-activated receptor-4 and purinergic receptor P2Y₁₂ dimerize, co-internalize, and activate Akt signaling via endosomal recruitment of β -arrestin. *Journal of Biological Chemistry*, 292(33), 13867–13878.
- Sriram, K., & Insel, P. A. (2018). GPCRs as targets for approved drugs: How many targets and how many drugs? *Molecular Pharmacology*, 93, 251–258.
- Swaminath, G., Deupi, X., Lee, T. W., Zhu, W., Thian, F. S., Kobilka, T. S., & Kobilka, B. (2005). Probing the β_2 Adrenoceptor Binding Site with Catechol Reveals Differences in Binding and Activation by Agonists and Partial Agonists. *The Journal of Biological Chemistry*, 280, 22165-22171.
- Tabor, A., Weisenburger, S., Banerjee, A., Purkayastha, N., Kaindl, J. M., Hübner, H., . . . Gmeiner, P. (2016). Visualization and ligand-induced modulation of dopamine receptor dimerization at the single molecule level. *Scientific Reports*, 6.
- Terrillon, S., Barberis, C., & Bouvier, M. (2004). Heterodimerization of V1a and V2 vasopressin receptors determines the interaction with β -arrestin and their trafficking patterns. *PNAS*, 101(6), 1548-1553.
- Venkatakrishnan, A., Flock, T., Prado, D. E., Oates, M. E., Gough, J., & Babu, M. (2014). Structured and disordered facets of the GPCR fold. *Current Opinion in Structural Biology*, 27, 129-137.
- Vischer, H. F., Castro, M., & Pin, J.-P. (2015). G Protein–Coupled Receptor Multimers: A Question Still Open Despite the Use of Novel Approaches. *Molecular Pharmacology*, 88(3), 561-571.

- Vogel, R., Mahalingam, M., Lüdeke, S., Huber, T., Siebert, F., & Sakmar, T. P. (2008). Functional Role of the “Ionic Lock”—An Interhelical Hydrogen-Bond Network in Family A Heptahelical Receptors. *Journal of Molecular Biology*, 380(4), 648-655.
- Wacker, D., Stevens, R. C., & Roth, B. L. (2017). How Ligands Illuminate GPCR Molecular Pharmacology. *Cell*, 170(3), 414-427.
- Wenzel-Seifert, K., & Seifert, R. (2000). Molecular analysis of beta(2)-adrenoceptor coupling to G(s)-, G(i)-, and G(q)-proteins. *Molecular Pharmacology*, 58(5), 954-966.
- White, J. F., Grodnitzky, J., Louis, J. M., Trinh, L. B., Shiloach, J., Gutierrez, J., . . . Grisshammer, R. (2007). Dimerization of the class A G protein-coupled neurotensin receptor NTS1 alters G protein interaction. *PNAS*, 104(29), 12199–12204.
- White, J. H., Wise, A., Main, M. J., Green, A., Fraser, N. J., Disney, G. H., . . . Marshall, F. H. (1998). Heterodimerization is required for the formation of a functional GABA_B receptor. *Nature*, 396, 679 – 682.
- Whorton, M. R., Bokoch, M. P., Rasmussen, S. G. F., Huang, B., Zare, R. N., Kobilka, B., & Sunahara, R. K. (2007). A monomeric G protein-coupled receptor isolated in a high-density lipoprotein particle efficiently activates its G protein. *Proceedings of the National Academy of Sciences of the United States of America*, 104(18), 7682–7687.
- Woulfe, D., Jiang, H., Morgans, A., Monks, R., Birnbaum, M., & Brass, L. F. (2004). Defects in secretion, aggregation, and thrombus formation in platelets from mice lacking Akt2. *The Journal of Clinical Investigation*, 113(3), 441–450.
- Woulfe, D. S. (2010). Akt signaling in platelets and thrombosis. *Expert Review of Hematology*, 3(1), 81–91.
- Xiang, B., Zhang, G., Liu, J., Morris, A. J., Smyth, S. S., Gartner, T. K., & Li, Z. (2010). A G_i-independent mechanism mediating Akt phosphorylation in platelets. *Journal of Thrombosis and Haemostasis*, 8(9), 2032–2041.
- Youker, R. T., & Teng, H. (2014). Measuring protein dynamics in live cells: protocols and practical considerations for fluorescence fluctuation microscopy. *Journal of Biomedical Optics*, 19(9).

- Zacharias, D. A., Violin, J. D., Newton, A. C., & Tsien, R. Y. (2002). Partitioning of Lipid-Modified Monomeric GFPs into Membrane Microdomains of Live Cells. *Science*, 296 (5569), 913-916.
- Zhang, J., Zhang, K., Gao, Z.-G., Paoletta, S., Zhang, D., Han, G. W., . . . Zhao, Q. (2014a). Agonist-bound structure of the human P2Y12 receptor. *Nature*, 509(7498), 119-122.
- Zhang, K., Zhang, J., Gao, Z.-G., Zhang, D., Zhu, L., Han, G. W., . . . Zhao, Q. (2014b). Structure of the human P2Y12 receptor in complex with an antithrombotic drug. *Nature*, 509(7498), 115-118.